Comprehensive genome-wide analysis and expression pattern profiling of the SlHVA22 gene family unravels their likely involvement in the abiotic stress adaptation of tomato

Antt Htet Wai
Sunchon National University
Muhammad Waseem
University of Narowal
Lae-Hyeon Cho
Pusan National University
Sang Tae Kim
The Catholic University of Korea
Do-jin Lee
Sunchon National University
Chang-Kil Kim
Kyungpook National University
Mi-Young Chung (queen@sunchon.ac.kr)
Sunchon National University

Research Article

Keywords: HVA22 genes, Solanum lycopersicum, Stress response, Subcellular localization, Gene co-expression network, 3D structure, Expression analysis

Posted Date: May 12th, 2022

DOI: https://doi.org/10.21203/rs.3.rs-1626245/v1

Abstract

Background: HVA22 family proteins with a conserved TB2/DP1/HVA22 domain are ubiquitous in eukaryotes. *HVA22* family genes have been identified in a variety of plant species. However, there has been no comprehensive genome-wide analysis of *HVA22* family genes in tomato (*Solanum lycopersicum* L.).

Results: In the present study, we identified 15 non-redundant *SlHVA22* genes with three segmentally duplicated gene pairs on 8 of the 12 tomato chromosomes. The predicted three-dimensional (3D) models and gene ontology (GO) annotations of SlHVA22 proteins pointed to their putative transporter activity and ability to bind to diverse ligands. The co-expression of *SlHVA22* genes with various genes implicated in multiple metabolic pathways and localization of SlHVA22-GFP fused proteins to the endoplasmic reticulum suggested that they might have a variety of biological functions, including vesicular transport in stressed cells. Comprehensive expression analysis revealed that *SlHVA22* genes were differentially expressed in various organs and in response to abiotic stress conditions. The predominant expression of *SlHVA22i* at the ripening stage and that of *SlHVA22g*, *SlHVA22k* and *SlHVA22l* in fruits at most developmental stages suggested their probable involvement in tomato fruit development and ripening. Moreover, transcript expression of most tomato *HVA22* genes, particularly *SlHVA22b*, *SlHVA22i*, *SlHVA22k*, *SlHVA22l*, *SlHVA22m* and *SlHVA22n*, was affected by abscisic acid (ABA) and diverse abiotic stress treatments, indicating the likely involvement of these genes in tomato abiotic stress responses in an ABA-dependent manner.

Conclusions: Overall, our findings provide a foundation to better understand the structures and functional roles of *SlHVA22* genes, many of which might be useful to improve the abiotic stress tolerance and fruit quality of tomato through marker-assisted backcrossing or transgenic approaches.

Background

TB2/DP1/HVA22 family proteins are prevalent in eukaryotes, such as plants, fungi, animals, and protozoa, but have not yet been identified in prokaryotes [1–3]. The plant HVA22 protein shares a high sequence similarity with the human TB2/DP1 protein. HVA22 was first identified as an abscisic acid (ABA)- and stress-induced gene from barley (*Hordeum vulgare*) [4]. Transmembrane domains critical for the proper localizations and functions of HVA22 proteins, such as regulation of programmed cell death in aleurone cells and vesicular trafficking in stressed cells, are prevalent in the TB2/DP1/HVA22 domain regions of HVA22 family members [1, 5, 6]. To date, over 355 HVA22 homologous proteins have been identified in eukaryotes, and the TB2/DP1/HVA22 domain is highly conserved in all of them [1].

Yop1p, identified in yeast, is homologous to HVA22 and capable of interacting with diverse proteins, including the endoplasmic reticulum (ER) resident protein Rtn4/NogoA, to regulate protein interactions and ER functions [7, 8]. The interaction of Yop1p and Sey1p during vesicular trafficking was elucidated by the agglomeration of transport vesicles and the reduction in invertase secretion in the yeast *yop1/sey1* double mutant [5]. mRNA accumulation of *Yop1* is induced under salt treatment, and *yop1* mutants also show sensitivity to mild temperature stress compared with the control [3, 5]. *HVA22* induced by ABA regulates seed germination and seedling growth by modulating vesicular trafficking in barley aleurone cells [1, 5]. Plant *HVA22* homologous genes responsive to environmental stresses harbor *cis*-regulatory elements associated with stress-related hormones and stress tolerance in their promoters [6, 9–11]. The interaction between the *cis* elements in the *HVA22* promoter and ABA- and stress-related genes has been verified in several plant species [12–15].

Plants as sessile organisms are occasionally exposed to unfavorable environmental conditions during growth and development. Abiotic stressors, including heat, cold, drought and salinity, have a profound effect on the growth and development of plants, resulting in significant crop yield losses worldwide [16]. Diverse abiotic stresses differentially regulate the expression of *HVA22* homologs in various plant species [3, 17, 18]. *HVA22* family members identified in *Arabidopsis* are differentially expressed on exposure to the plant stress hormone ABA and abiotic stresses [17]. The introgression of stress-related genes under the control of the *HVA22* promoter as a stress-inducible promoter in rice enhances drought tolerance of the resulting rice transgenic lines compared with wild-type (WT) plants [19]. Six *CcHVA22* homologs have been identified in two citrus species (*Citrus sinensis* and *Citrus clementina*), and *CcHVA22d*-overexpressing tobacco transgenic lines display tolerance to dehydration and oxidative stress [6]. The *HVA22* homolog from halophytic cordgrass (*Spartina alterniflora*) displays varied transcript levels on exposure to different salinity levels [18]. Likewise, the tomato *HVA22* homolog (referred to as *SlHVA22n* here) is significantly induced by salt treatment in the tomato (*Solanum lycopersicum* L.) cultivar Micro-Tom. It is also upregulated in *LeERF1*- and *LeERF2*-overexpressing tomato plants tolerant to salt stress compared with WT plants [20].

Tomato is a commercially valuable fruit crop as well as a fleshy fruit model plant used to study the mechanisms of fruit ripening. Different unfavorable environmental conditions significantly reduce the productivity and fruit quality of tomato [16]. Therefore, extensive research has been conducted to better understand the molecular pathways controlling fruit development and ripening of tomato and to maximize fruit yield and quality under environmental stresses. In this study, we analyzed the expression profiles of the tomato *HVA22* gene family at different developmental stages, including five fruit developmental stages, and under diverse abiotic stress treatments. We conducted systematic and comprehensive genome-wide characterization as well as phylogenetic and gene co-expression network analyses. Finally, we determined the subcellular localization of *SlHVA22* genes. Our results will provide a solid foundation for future functional elucidation of potential tomato *HVA22* genes related to development and abiotic stress tolerance of tomato.

Results

In silico identification of tomato HVA22 family proteins

We identified 15 *HVA22* tomato genes and designated them as *HVA22a– HVA22o* based on their chromosomal locations. In silico analysis revealed significant variation in the lengths of open reading

Table 1

In silico analysis of the *HVA22* genes and corresponding proteins in tomato genome

Gene Name	Locus name	ORF (bp)	Chromosome No.	Protein					Subcellular Localization	No. of Introns
				Length (aa)	TB2/DP1/HVA22 domain Start-End (aa)	MW (kDa)	PI	GRAVY		
SlHVA22a	Solyc01g007780	663	1	220	19-97	25.80	9.35	-0.510	Nucleus	4
SlHVA22b	Solyc03g097420	411	3	136	24-98	15.84	9.37	0.210	Extracellular	4
SlHVA22c	Solyc03g110920	585	3	194	42-118	21.79	6.37	0.111	Endoplasmic reticulum	7
SlHVA22d	Solyc03g116350	531	3	176	32-107	20.50	6.41	0.005	Extracellular	4
SlHVA22e	Solyc04g014420	333	4	110	5-77	13.04	5.34	-0.034	Cytoplasm	2
SlHVA22f	Solyc04g076610	1410	4	469	32-108	53.34	9.03	-0.147	Nucleus	4
SlHVA22g	Solyc04g081340	915	4	304	19-96	33.64	8.95	-0.389	Chloroplast	4
SlHVA22h	Solyc05g007300	516	5	171	28-104	20.24	7.67	-0.101	Endoplasmic reticulum	4
SlHVA22i	Solyc06g072680	408	6	135	24-98	15.66	8.80	0.210	Chloroplast	4
SlHVA22j	Solyc10g007820	471	10	156	24-98	18.03	9.26	0.026	Chloroplast	4
SlHVA22k	Solyc10g047670	1680	10	559	24-100	63.67	8.73	-0.449	Nucleus	7
SlHVA22l	Solyc10g051300	564	10	187	32-108	21.86	7.02	-0.092	Endoplasmic reticulum	6
SlHVA22m	Solyc10g082040	570	10	189	19-97	22.23	8.84	-0.215	Extracellular	4
SlHVA22n	Solyc11g010930	429	11	142	24-98	16.85	8.58	0.065	Cytoplasm	2
SlHVA22o	Solyc12g089290	372	12	314	31-108	35.11	9.38	-0.399	Chloroplast	1

ORF, open reading frame; bp, base pair; aa, amino acid; kDa, kilo Dalton; pI, isoelectric point; MW, molecular weight; GRAVY, Grand average of hydropathicity.

frames of the *SlHVA22* genes, ranging between 333 bp (*SlHVA22e*) and 1680 bp (*SlHVA22k*), with a mean of 657 bp. The lengths of SlHVA22 proteins ranged from 110 to 559 amino acids (aa) for SlHVA22e and SlHVA22k, respectively, with a mean of 231 aa. The predicted molecular weights varied from 13.04 to 63.67 with iso-electric points (pI) of 5.34 to 9.38, which indicated that certain SlHVA22s were acidic, whereas others were basic. The grand average of hydropathicity (GRAVY) ranged from − 0.510 to 0.210, revealing that the computed HVA22s included both hydrophilic and hydrophobic proteins (Table 1). The protein sequence identity ranged from 10–73% among SlHVA22 proteins, and the proteins that clustered in the same phylogenetic groups had higher sequence identities than those from different groups (Table S4).

Phylogenetic analysis of HVA22 proteins

The phylogenetic analysis classified diverse plant HVA22 family proteins into two major clades, which were further divided into four groups according to their phylogenetic relationship (Fig. 1). The 15 tomato HVA22s were distributed in all four groups, with the largest number of proteins (SlHVA22d, SlHVA22f, SlHVA22h, SlHVA22j and SlHVA22k) in group I and the smallest number (SlHVA22c and SlHVA22l) in group III. The other two groups had four proteins: Group II contained SlHVA22b, SlHVA22e, SlHVA22i and SlHVA22n, and group IV contained SlHVA22a, SlHVA22g, SlHVA22m and SlHVA22o. All SlHVA22 members preferentially clustered with their homologs from potato, which is an evolutionarily closely related species, except SlHVA22j, which was in the same cluster with the homologs from rice and sorghum. The HVA22 members from the basal angiosperm *Amborella trichopoda* were distributed in all four groups and clustered with their monocot homologs in group I but paired with the homologs from dicotyledonous species citrus and *Arabidopsis* in groups II and IV, respectively. In contrast, the corresponding proteins from the moss *Physcomitrella patens* and the green alga *Chlamydomonas reinhardtii* were only in groups II and III. The moss homologs were distributed evenly in both groups, with six in group II and seven in group III, while those of the unicellular green alga were unevenly distributed, with one in group II and three in group III.

Gene structure, conserved motif and domain analysis of tomato HVA22 **genes**

Analysis of the exon–intron organization revealed structural divergence in the tomato *HVA22* gene family (Fig. S1). The number of exons in the *SlHVA22* members varied from two to eight with a mean of five. However, the exon–intron composition of most *HVA22* genes in the same phylogeny group was identical or similar, highlighting the structural similarity within phylogenetically closely related members. Likewise, the majority of the SlHVA22 homologs clustered together in the same phylogenetic clades contained similar conserved motif organization, indicating structural similarity among phylogenetically closely related members (Figs. S2 and S3). We also identified several motifs unique to some HVA22 members, such as motif 6 for SlHVA22g and SlHVA22o, motif 10 for SlHVA22c and SlHVA22l and motif 7 for SlHVA22d and SlHVA22h. The conserved motifs identified were similar in the homologous proteins clustered in the same phylogenetic groups from all three plant species (*Arabidopsis*, tomato and rice), implying they are highly conserved in dicots and monocots. Motifs 1 and 2 were located in the TB2/DP1/HVA22 domain and were present in all HVA22 homologous proteins from *Arabidopsis*, tomato and rice, except for OsHVA22b, indicating that these important motifs were evolutionarily conserved in both dicot and monocot plants. The domain architecture of *SlHVA22* genes was diverse, varying from the presence of the single TB2/DP1/HVA22 domain to the composition of other additional domains such as transmembrane domains, ZnF_U1 domains, ZnF_C2H2 domains, and RVT_3 domains (Fig. 2). The TB2/DP1/HVA22 domains with a length of 77–79 aa in tomato HVA22 proteins were highly conserved and started with the conserved Pro residue (except SlHVA22e that started with Cys residue). The transmembrane domains (TMDs) present in most tomato HVA22 members were composed of 23 aa residues, except in a few TMDs that varied from 18 to 20 aa. Other types of domains (ZnF_U1, ZnF_C2H2 and RVT_3) were identified only in SlHVA22f and SlHVA22k. Analysis of the multiple sequence alignment of the TB2/DP1/HVA22 domain of SlHVA22 family members with that of the human homolog TB2/DP1 protein revealed the evolutionary conservation of HVA22 family proteins from a human and a dicotyledonous plant, including the conservation of the casein kinase II (CKII) phosphorylation sites ([S/T]XX[D/E]) in the third α-helices of the domain (Fig. 3)[3].

Chromosomal position, gene duplication, and microsynteny analysis of SlHVA22 **genes**

SlHVA22 genes were unevenly situated in 8 of the 12 chromosomes (Chr) of tomato, and most of them were located close to the distal portions of the chromosomes (Fig. S4). Five of these chromosomes (Chr 1, 5, 6, 11 and 12) carried only one gene each, while Chr 3 and 4 harbored three and Chr 10 harbored four genes. Three segmentally duplicated gene pairs (*SlHVA22a*/ *SlHVA22m*, *SlHVA22e*/ *SlHVA22n* and *SlHVA22g*/ *SlHVA22o*) were predicted in tomato, two of which belonged to phylogenetic group IV, whereas the remaining pair belonged to group II (Figs. 1 and Fig. S5). The duplicated genes of each pair were located on different chromosomes, one of which carried only a single *SlHVA22* gene, while the other had three or four *SlHVA22* genes. Tandem duplication events were not detected because the genes were not mapped within the 100-kb region on the same chromosome. The Ka/Ks ratio of all the duplicated gene pairs in the tomato *HVA22* gene family was less than one, revealing that these genes have been influenced by intense purifying selection over the course of evolution (Table 2). We estimated that these duplicated gene pairs diverged 13.77–25.2

Table 2
Predicted Ka/Ks ratio of the duplicated SlHVA22 gene pair along with its divergence time

Duplicated gene pair			Ka	Ks	Ka/Ks	Duplication type	Types of selection	Time (MYA)
SlHVA22a	vs.	*SlHVA22m*	0.256048578	0.755904898	0.338731206	Segmental	Purifying selection	25.20
SlHVA22e	vs.	SlHVA22n	0.190039202	0.413123219	0.460006102	Segmental	Purifying selection	13.77
SlHVA22g	vs.	SlHVA22o	0.183462269	0.580908552	0.315819535	Segmental	Purifying selection	19.36

Ks, the number of synonymous substitutions per synonymous site; Ka, the number of non-synonymous substitutions per nonsynonymous site; MYA, million years ago

Ks, the number of synonymous substitutions per synonymous site; Ka, the number of non–synonymous substitutions per nonsynonymous site; MYA, million years ago

million years ago. We conducted a comparative microsynteny analysis to determine *HVA22* orthologous gene pairs among *Arabidopsis*, tomato and rice to discern the evolutionary correlation across their genomes (Fig. 4). We identified four orthologous gene pairs between *Arabidopsis* and tomato, whereas there were no orthologous gene pairs between *Arabidopsis* and rice or tomato and rice.

Prediction of cis**-regulatory elements, microRNA (miRNA) target sites and phosphorylation sites**

Hormonal regulation of gene expression is also vital in the control of stress responses in plants [21]. We identified many *cis*-regulatory elements related to phytohormones and abiotic stress responses in the promoter regions of tomato *HVA22* genes. These included ABA-responsive elements; TGACG and CGTCA motifs (with roles in the jasmonic acid response); TCA elements (related to the salicylic acid response); P-box, GARE and TATC elements associated with the gibberellic acid response; auxin response-related TGA-box and TGA elements; MYB-binding site and MYB elements responsive to drought; low temperature-responsive elements with roles in low temperature and hypersalinity stress and defense; and stress response-related TC-rich repeats (Fig. S6 and Table S5). miRNAs function in the regulation of biotic and abiotic stress tolerance in plants by targeting a wide range of stress-related genes [22, 23]. We identified many miRNA target sites related to abiotic stress tolerance in tomato in most *HVA22* genes, except *SlHVA22e*, *SlHVA22h*, and *SlHVA22i* (Table S6). Nineteen miRNA target sites involved in abiotic stress tolerance in tomato were predicted in 11 *SlHVA22* genes. Post-translation regulation of stress-related proteins via phosphorylation is common and important in plant stress responses. We identified numerous phosphorylation sites, including the sites targeted by CKII and several N-glycosylation sites, in tomato HVA22 proteins (Table S7).

Comparative modelling of tomato SlHVA22 proteins

The predicted 3D models indicated that the TB2/DP1/HVA22 domain (77–79 aa) was present as a 3D frame comprised mainly of α-helixes in all tomato HVA22 proteins, most of which were only composed of α-helixes and coils, while a few (SlHVA22f, SlHVA22k and SlHVA22o) also included β-sheets (Fig. 5). The number of secondary structural components of tomato HVA22 proteins was 4–22 for α-helixes, 0–9 for β-sheets and 5–27 for coils (Table S8). The number of secondary structural components was highly conserved in most tomato proteins with only 4 or 6 α-helixes and 5 or 7 coils,

whereas only two proteins had more α-helixes and coils (13 and 22 for HVA22f, respectively, and 22 and 27 for SlHVA22k, respectively). Only 3 of 15 predicted models contained β-sheets (2 for HVA22o, 4 for HVA22k and 9 for SlHVA22f). The C-scores and TM-scores along with other parameters of all the predicted models that were within a reasonable range are described in Tables S9 and S10 to indicate the validity of the constructed models [24]. We identified the putative ligand-binding sites capable of interacting with diverse molecules in all predicted models. We predicted the molecular functions of SlHVA22 family members, including binding ability to a variety of ligands, transporter activity and transferase activity, based on gene ontology (GO) terms using the I-TASSER server (Table S11).

Gene co-expression network analysis

We determined the co-expression profiles of *SlHVA22* genes using RNA sequencing data with weighted gene co-expression network analysis and showed that 263 genes were co-expressed with *SlHVA22* genes (Fig. 6). The hub genes (*SlHVA22a*, *SlHVA2g*, *SlHVA22k* and *SlHVA22l*) were co-expressed with 111, 107, 23 and 22 genes, respectively. In the GO and Kyoto Encyclopedia of Genes and Genomes enrichment results, certain genes present in the co-expression network were not annotated with any biological process, but most genes were engaged in a variety of biological pathways, including environmental information processing, signaling and cellular processes, nucleic acid binding, oxidative phosphorylation, starch and sucrose metabolism, transport and catabolism, biosynthesis of secondary metabolites, membrane transport, lipid metabolism, metabolism of amino acids, mRNA metabolism and phosphorus metabolic processes (Figs. 6 and 7, Fig. S7 and Table S12).

Genes related to development and abiotic stress responses of tomato were identified in the co-expression network. Numerous genes responsive to diverse abiotic stresses and/or expressed in roots were co-expressed with *SlHVA22a*. We also identified several genes that were responsive to abiotic stresses and/or expressed in fruits in the co-expression networks of *SlHVA22g*, *SlHVA22k* and *SlHVA22l*.

Subcellular localization of SlHVA22 proteins

The predicted localization analysis showed that tomato HVA22 proteins were localized to various parts of the cell, including the ER, chloroplasts and nucleus (Table S13). Further determination of subcellular locations of SlHVA22 proteins through the expression of these proteins fused with GFP in the rice protoplasts indicated that SlHVA22a, SlHVA22f, SlHVA22k and SlHVA22n were predominantly localized in the ER (Fig. 8).

Expression profiling of tomato HVA22 genes in different organs

The expression profiles of *SlHVA22* genes in tomato organs revealed differential expression patterns in all tested organs (Fig. 9). We determined expression levels in various organs relative to that in leaves (control). The duplicated gene pair *SlHVA22a* and *SlHVA22m* had high relative expression levels in roots (4- and > 5-fold higher than the control, respectively). *SlHVA22m* was the only gene whose expression was not detected in young (1-cm) or immature (IM) fruit. *SlHVA22b*, *SlHVA22h* and *SlHVA22j* had higher relative expression in stems than in other vegetative and reproductive organs (> 20-, 14- and 2-fold higher, respectively, than in the control), but the peak expression of *SlHVA22h* in stems was similar to that in leaves and flowers. *SlHVA22d* is the only gene whose expression was highest in leaves followed by mature green (MG) fruit, IM fruit and fruit 5 d after the breaker stage (B5), respectively. *SlHVA22f* and *SlHVA22o* had higher relative expression in flowers compared to in other organs (> 2- and ~ 2-fold higher, respectively, than in the control). *SlHVA22c* had a ~ 2-, ~ 1.9- and 1.7-fold higher expression level in IM fruit, stems and B5 fruit relative to the control, respectively. *SlHVA22k* had the highest expression level in MG fruit (2.6-fold higher than in the control) followed by IM fruit, B5 fruit and fruit at the breaker stage (B), respectively. *SlHVA22n* was predominantly expressed in MG fruit (~ 4.7-fold higher expression than in the control); it also showed a > 4-fold higher expression in flowers and roots compared with the control. *SlHVA22i* was preferentially expressed in B5 fruit (> 290-fold higher expression than the control) and in B fruit (> 80-fold higher than the control). *SlHVA22g* exhibited an ~ 2-fold higher expression level in B5 fruit than in the control and was also highly expressed in B and IM fruit. *SlHVA22l*, whose expression peaked in B5 fruit (when it was 3.5-fold higher than that in control), displayed higher expression in the cell expansion (IM and MG) and ripening (B and B5) stages of tomato compared with other organs.

Expression analysis of SlHVA22 genes in response to abiotic stresses and phytohormone treatment

We determined the transcript profiles of tomato *HVA22* gene family members in leaf samples exposed to different abiotic stresses (cold, heat, drought and salt) and phytohormone (ABA) treatment via a qRT-PCR assay. Many *SlHVA22* genes were differentially expressed in response to these stress treatments (Fig. 10a and b).

Nine genes (*SlHVA22c*, *SlHVA22d*, *SlHVA22f*, *SlHVA22g*, *SlHVA22h*, *SlHVA22k*, *SlHVA22l*, *SlHVA22m* and *SlHVA22o*) were significantly downregulated by cold stress (1.4- to 12-fold lower expression compared with that in the control [0 h sample]). In contrast, five genes (*SlHVA22a*, *SlHVA22b*, *SlHVA22e*, *SlHVA22i* and *SlHVA22n*) were significantly upregulated by 1.4- to 7.8-fold under cold stress. Of these, *SlHVA22i* and *SlHVA22n* were upregulated by > 6- and 7-fold, respectively, compared with the control. *SlHVA22j* was the only gene not responsive to cold treatment (Fig. 10a).

All tomato *HVA22* genes displayed heat stress responses. Eleven genes (*SlHVA22b*, *SlHVA22c*, *SlHVA22d*, *SlHVA22e*, *SlHVA22g*, *SlHVA22i*, *SlHVA22j*, *SlHVA22k*, *SlHVA22l*, *SlHVA22m* and *SlHVA22o*) were significantly upregulated by heat stress in comparison with the control (by 1.9- to 16.5-fold). In particular, the transcript levels of *SlHVA22b*, *SlHVA22g*, *SlHVA22l* and *SlHVA22o* were upregulated by > 3-fold and those of *SlHVA22i* by > 16-fold in response to heat treatment. In contrast, four genes (*SlHVA22a*, *SlHVA22f*, *SlHVA22h* and *SlHVA22n*) were downregulated (by 1.9- to 2.5-fold) under heat treatment (Fig. 10a).

Drought treatment also affected the expression levels of all *SlHVA22* genes. *SlHVA22i* expression was upregulated by 1.87- to 126-fold at all stages of drought stress in comparison to the control, most prominently at 3–24 h of treatment. Likewise, *SlHVA22k*, *SlHVA22l* and *SlHVA22n* were upregulated by 1.4- to 8.5-fold under all drought stress time points. The expression of *SlHVA22a*, *SlHVA22c* and *SlHVA22d* was highest (upregulated by 1.4- to 1.6-fold) at 1 h under drought treatment, while that of *SlHVA22g* peaked (upregulated by ~ 1.6-fold) at 9 h following exposure to drought. On the other hand, *SlHVA22e*, *SlHVA22f*, *SlHVA22h*, *SlHVA22j* and *SlHVA22o* were significantly downregulated by 1.6- to 17-fold at 3–24 h after drought treatment. *SlHVA22b* was downregulated by drought but only at the early stage, while *SlHVA22m* was downregulated by 1.6- to 2.7-fold at 3 and 9 h, respectively, after exposure to drought treatment (Fig. 10a).

Salt treatment either markedly up- or downregulated most *SlHVA22* genes in comparison to the control, except for *SlHVA22j*, which was only minimally up- or downregulated (by ~ 1.3-fold). Eleven of the fifteen genes (*SlHVA22a*, *SlHVA22b*, *SlHVA22c*, *SlHVA22e*, *SlHVA22f*, *SlHVA22g*, *SlHVA22i*, *SlHVA22k*, *SlHVA22l*, *SlHVA22m* and *SlHVA22n*) were significantly upregulated by 1.6- to 63-fold under cold stress in comparison with the control. Among the upregulated genes, the expression of *SlHVA22m*, *SlHVA22i*, *SlHVA22b*, *SlHVA22n* and *SlHVA22l* was upregulated by 63-, 16-, 9-, 6-, and 3-fold compared with the control, respectively, under exposure to saline conditions. However, a few genes (*SlHVA22h*, *SlHVA22j* and *SlHVA22o*) were downregulated by 1.8- to 3.3-fold under salt stress compared with the control (Fig. 10b).

The transcription of many tomato *HVA22* genes, apart from *SlHVA22d*, was affected by ABA stress hormone treatment. *SlHVA22o* was downregulated (by ~ 1.3-fold) at all time points, and *SlHVA22j* was downregulated (by 1.4-fold) at the last time point of ABA treatment compared with the control. In contrast, many genes (*SlHVA22a*, *SlHVA22c*, *SlHVA22e*, *SlHVA22g*, *SlHVA22h*, *SlHVA22k* and *SlHVA22l*) were upregulated by 1.4- to 1.8-fold under ABA treatment compared with the control. *SlHVA22i* was upregulated by 1.9- to > 7-fold under ABA treatment at all time points compared with the control. *SlHVA22f* was significantly upregulated by 2.2- to 4.7-fold under exposure to ABA at the early stages of treatment. Similarly, the expression of *SlHVA22b* was upregulated by 1.8- to 2-fold at the early stages of ABA treatment, while that of *SlHVA22b* peaked at 9 h after treatment, when it was 3-fold higher than that in the control (Fig. 10b).

Discussion

This is the first comprehensive study of *HVA22* genes in a solanaceous crop species. We identified and comprehensively characterized 15 non-redundant *SlHVA22* genes at a genome-wide scale. As in other flowering plant species, the existence of *HVA22* genes as a multiple gene family in tomato (Fig. 1) suggested their important biological role in this model fruit crop. TB2/DP1/HVA22 family proteins have been identified in eukaryotes but not in prokaryotes, indicating that they might have evolved after the divergence of prokaryotes and eukaryotes, playing a vital role in eukaryote evolution.

We performed a phylogenetic analysis to explore the evolutionary relationship among HVA22 homologs from diverse species in the plant kingdom. The phylogenetic tree depicted a major clustering of proteins from dicots (*Arabidopsis*, citrus, tomato and potato) and monocots (rice, maize and sorghum) along with lower plants (Fig. 1). The corresponding proteins from the moss *Physcomitrella patens* and the single-celled green alga *Chlamydomonas reinhardtii* only occurred in phylogenetic groups II and III, revealing that the HVA22 proteins from these two phylogenetic groups (II and III) were more primitive than proteins in other groups (I and IV) and may have evolved from the common ancestor of chlorophytes and streptophytes, which diverged over one billion years ago [25]. The prevalence of only the HVA22 homologs from angiosperms in groups I and VI indicated that the homologs from these phylogenetic groups may have evolved before the divergence of monocots and dicots (~ 200 million years ago) [26].

All *HVA22* genes in the *Citrus* species contain TMDs (Ferreira et al., 2019); however, *SlHVA22* genes varied in terms of absence or presence of different numbers of TMDs (Fig. 2). This domain organization may play a role in the structural and functional divergence of *HVA22* genes in tomato. In addition, *SlHVA22* genes contained other types of domains, such as zinc-finger domains identified in DNA- and RNA-binding proteins (C2H2-type zinc-finger domain, U1-type zinc-finger domain) and RVT_3 domains in a few tomato genes. The domains may have also enhanced the diversification of the tomato *HVA22* gene family. The conserved motifs, exons and introns identified in *SlHVA22* gene family members were arranged in a similar manner across evolutionarily closely related *SlHVA22* genes but in a dissimilar arrangement from those of different phylogenetic groups (Figs. S1 and S2). This could explain the functional similarity among evolutionarily closely related *SlHVA22* genes and the functional dissimilarity across divergent ones over the course of evolution.

Three segmentally duplicated gene pairs (*SlHVA22a*/ *SlHVA22m*, *SlHVA22e*/ *SlHVA22n* and *SlHVA22g*/ *SlHVA22o*) were predicted in tomato (Fig. S5 and Table 2). Therefore, *HVA22* family members might have evolved from an original set of 12 progenitor genes in tomato. The duplicated genes of each pair resided on different chromosomes, one of which contained only one *HVA22* gene, whereas the others had three or four *HVA22* genes (Fig. S3), suggesting that gene duplication increased not only the number of *HVA22* genes in the tomato genome but also the number of chromosomes carrying them in tomato. This result indicates that more chromosomes in tomato may have needed to harbor *HVA22* genes during evolution to boost important biological functions in tomato cells such as adaptation to unfavorable environmental conditions.

A comparative microsyntenic map constructed to explore the evolutionary relationship among *HVA22* orthologs from *Arabidopsis*, tomato and rice revealed four pairs of orthologous genes between *Arabidopsis* and tomato but none between rice and *Arabidopsis* or tomato (Fig. 4). These results are well correlated with the closer evolutionary connection of tomato with *Arabidopsis* than with rice and also suggest that four *SlHVA22* genes might have derived from *Arabidopsis* during species divergence.

Cis-acting elements in the promoter sequences of genes can act like circuit breakers to switch on and off the transcription of their genes upon exposure to different environmental stimuli [27, 28]. The presence of several *cis*-regulatory elements related to hormonal and abiotic stress responses upstream of tomato *HVA22* genes highlighted their probable roles in tomato abiotic stress tolerance (Fig. S6). This result is corroborated by the prevalence of hormonal and stress-related *cis* elements, which can interact with diverse *trans*-acting genes, including stress-related transcription factors, in the promoter regions of stress-induced *HVA22* genes in other plant species [1, 3, 6, 13, 17].

To determine whether the abiotic stress responses of *SlHVA22* genes could also be related to miRNAs, we analyzed the miRNA target sites in *SlHVA22* genes. Eleven out of fifteen *SlHVA22* gene family members were targeted by tomato miRNAs that regulate abiotic stress tolerance in tomato, such as *Sly-MIR159b*, *Sly-MIR166c-5p*, *Sly-MIR1917*, *Sly-MIR395a*, *Sly-MIR396a*, *Sly-MIR396a-5p*, *Sly-MIR482a*, *Sly-MIR5302a*, *Sly-MIR5303*, *Sly-MIR6023*, *Sly-MIR6024*, *Sly-MIR9470-5p*, *Sly-MIR9474-5p*, *Sly-MIR9479* and *sly-MIR9479-3p* [29–32] (Table S6). This indicates that many *SlHVA22* genes might be linked to the post-transcriptional regulation of miRNAs in tomato abiotic stress tolerance.

Protein phosphorylation, a crucial post-translational modification regulated by kinases and phosphatases, is crucial in signaling pathways and stress responses in plants [33, 34]. Prediction of phosphorylation sites using the NetPhos 3.1 Server revealed that many putative phosphorylation sites were prevalent in all tomato HVA22 proteins (Table S7), which is consistent with the distribution of phosphorylation sites in HVA22 homologs in other species [3, 4, 6].

The 3D structure of a protein can provide useful clues to predict its possible interaction with other molecules and its biological functions. Thus, we analyzed 3D models of tomato HVA22 proteins to gain a better understanding of their molecular structural conformations and putative functions. Most HVA22 proteins had similar numbers of α-helixes, β-sheets and coils (Table S8), suggesting structural conservation in most HVA22 family members during evolution. SlHVA22 proteins were predicted to harbor ligand-binding sites that interact with various molecules, such as ions, intracellular messengers or receptor molecules, to initiate a change in cell function. SlHVA22 proteins were also predicted to have various molecular functions, including the ability to bind to a variety of ligands, transporter activity and transferase activity based on the GO terms (Fig. 5 and Table S11). These results indicate that SlHVA22 proteins might have several important biological functions in tomato.

The determination of protein subcellular localization can indicate putative functions. Subcellular localization analysis revealed that tomato HVA22 proteins were predominantly localized to the ER (Fig. 8). This finding was consistent with the localization of HVA22 homologs from barley and yeast in the ER, suggesting that HVA22 homologs from diverse species might have a conserved function, such as vesicular trafficking in abiotic stress responses [1, 8].

A qRT-PCR assay revealed varied expression patterns of *SlHVA22* genes in the different organs tested, suggesting that they might have distinct regulatory functions in the growth and development of tomato (Fig. 9). Of the 15 tomato *HVA22* genes, 8 genes (*SlHVA22c*, *SlHVA22f*, *SlHVA22g*, *SlHVA22i*, *SlHVA22k*, *SlHVA22l*, *SlHVA22n* and *SlHVA22o*) had high transcript levels in reproductive organs (flowers or fruits), whereas 7 genes (*SlHVA22a*, *SlHVA22b*, *SlHVA22d*, *SlHVA22e*, *SlHVA22h*, *SlHVA22j* and *SlHVA22m*) had high transcript levels in vegetative organs, such as leaves, roots, or stems, hinting at their preferential roles in these organs and developmental stages in tomato.

The expression of *SlHVA22d* was highest in leaves, IM fruit, MG fruit and B5 fruit, pointing to its possible role in the growth of leaves and fruit. The roots play a vital role in the uptake of water and minerals for growth and development of plants. The mRNA transcript levels of *SlHVA22a* and *SlHVA22m* were highest in roots, suggesting their probable involvement in root growth and uptake of nutrients and water. The stem is the main organ that provides mechanical strength to the aerial parts of the plant and transports water and nutrients to promote plant growth and development under normal and unfavorable environmental conditions. The higher mRNA transcript accumulation of *SlHVA22b*, *SlHVA22e*, *SlHVA22h* and *SlHVA22j* in stems compared to in other organs hints at their likely role in stem development, long-range translocation of water and minerals as well as stress adaptation (Fig. 9).

Of the eight *SlHVA22* genes that were highly expressed in reproductive organs, two genes (*SlHVA22f* and *SlHVA22o*) were predominantly expressed in flowers, suggesting their probable role in flower development. Tomato, as a model fleshy fruit crop, has been widely studied to understand the regulatory mechanisms governing the growth and ripening of climacteric fruits [35–37]. The expression of *SlHVA22k* and *SlHVA22l* was higher in fruit at all fruit developmental stages, except at the 1-cm fruit stage, compared with in other organs. This result suggests that *SlHVA22k* and *SlHVA22l* may actively function throughout the developmental stages of fruit starting from the cell expansion phase. The mRNA transcript levels of *SlHVA22n* were higher in IM and MG fruit than in fruit at other developmental stages, suggesting its active role in the cell expansion phase of fruit development. *SlHVA22c* is the only gene whose expression peaked in IM fruit, indicating that it may influence the early cell expansion phase of tomato. The higher expression levels of

SlHVA22g in B and B5 fruit suggested its possible role in tomato fruit ripening. The transcript levels of *SlHVA22i* were high in B fruit (> 80-fold higher than in the control) and highest in B5 fruit (~ 300-fold higher than in the control). This finding indicates that *SlHVA22i* may be a novel gene implicated in the regulation of fruit ripening. The predominant expression of the duplicated gene pair (*SlHVA22a/SlHVA22m*) in the same organ (root) suggested functional conservation, whereas the differential expression levels of other duplicated gene pairs (*SlHVA22e/SlHVA22n* and *SlHVA22g/SlHVA22o*) in different organs suggested functional diversification after gene duplication (Fig. 9**)**.

Plant adaptation to diverse environmental stresses is regulated by gene networks, including transcription factors and downstream stress-related genes in ABA-dependent or -independent manners [38–41]. Previous studies have reported ABA- and stress-induced differential expression of *HVA22* gene family members in various plant species [3, 17, 18]; interactions between the *cis* elements located in the promoter regions of *HVA22* homologs with several ABA- and stress-related genes; and the exploitation of the *HVA22* promoter as a stress-inducible promoter of stress-related genes in transgenic plants [12–15, 19]. Therefore, it is likely that *SlHVA22* genes function in tomato abiotic stress tolerance.

In the current study, tomato *HVA22* genes displayed differential transcript levels upon exposure to abiotic stress stimuli (Fig. 10a and b). Most *SlHVA22* genes were significantly downregulated, while several genes were dramatically upregulated, and only one gene (*SlHVA22j*) was not responsive under cold treatment. This result agrees with a previous study reporting the cold-induced expression of barley *HVA22* gene and the differential responses of *Arabidopsis HVA22* homologs under cold stress conditions [13, 17]. The expression of *SlHVA22b*, *SlHVA22i* and *SlHVA22n* was highly induced following cold stress (Fig. 10a), suggesting their potential role in cold stress tolerance in tomato.

In contrast to cold stress, many *SlHVA22* genes were upregulated, whereas few genes (*SlHVA22a*, *SlHVA22f*, *SlHVA22h* and *SlHVA22n*) were downregulated by heat treatment. In response to heat stress, 11 of the 15 *SlHVA22* genes were upregulated, and *SlHVA22i* showed the highest expression (Fig. 10a). These genes may be crucial in tomato heat tolerance. These observations are corroborated by a previous study that determined that a mutation in *YOP1*, the yeast (*Saccharomyces cerevisiae*) *HVA22* homolog, results in a growth defect in *yop1* mutants under mild temperature stress (37°C) [5].

Drought treatment upregulated half of the tomato *HVA22* genes and downregulated the other half. *SlHVA22i* had the highest expression level in response to drought stress, followed by *SlHVA22n* (Fig. 10a). This suggests that *SlHVA22i* and *SlHVA22n* might actively function in the tomato drought response. These findings are consistent with a previous report in which the expression of *AtHVA22* homologs was differentially regulated by drought and another report in which *CcHVA22d*-overexpressing transgenic tobacco exhibited a lower dehydration rate and buildup of H_2O_2 than the WT [6, 17].

Under salt stress conditions, the transcript levels of most *SlHVA22* genes increased, but those of a few genes (*SlHVA22d*, *SlHVA22h* and *SlHVA22o*) decreased. Eleven *SlHVA22* genes were upregulated, with *SlHVA22m* having the greatest expression, followed by *SlHVA22i*, *SlHVA22b* and *SlHVA22n* (Fig. 10b). This indicates the potential involvement of these genes in the salt response of tomato. This is in agreement with previous studies reporting the salt-responsive expression of *HVA22* homologs in yeast and several plant species, and elevated mRNA transcripts of the tomato *HVA22* homolog (*SlHVA22n* in this study) in the salt-tolerant tomato *LeERF1* and *LeERF2* transgenic lines [3, 18, 20].

ABA is a well-studied phytohormone that regulates a variety of stress-related genes to promote plant tolerance to unfavorable environmental conditions such as cold, heat, drought and salt stress [42–44]. Except for *SlHVA22d*, the expression of all *SlHVA22* genes was altered by ABA treatment, with *SlHVA22i* exhibiting the highest expression, followed by *SlHVA22f* and *SlHVA22n* (Fig. 10b). This finding agrees with previous work reporting the responses of *HVA22* homologs from barley and *Arabidopsis* upon exposure to ABA, hinting at their functional role in abiotic stress adaptation in tomato in an ABA-dependent manner [4–17].

We performed a co-expression network analysis of *SlHVA22* genes using RNA sequencing data to further understand their putative functions in tomato. The genes co-expressed with *SlHVA22* genes were involved in diverse biological pathways including abiotic stress responses and development (Figs. 6 and 7, Fig. S7 and Table S12), suggesting the important biological role of *SlHVA22* genes in tomato. Multiple abiotic stress-responsive genes, such as *SlyHSF-24* (Solyc09g009100), *SlDEAD22* (Solyc07g042010) and *SlDEAD29* (Solyc09g090740) [45–47], were co-expressed with *SlHVA22a*, which is in agreement with our finding that *SlHVA22a* responded to abiotic stress treatment. In addition, *SlPIP1;5* (Solyc08g081190), which was highly expressed in roots and under salt treatment, was co-expressed with *SlHVA22a*, whose expression peaked in roots and on exposure to salt stress [48], suggesting that these genes might interact with each other in the root development and salt tolerance of tomato.

We also identified several genes in the co-expression networks that were related to abiotic stress responses and/or expressed in fruits, such as *SPS1* (Solyc07g007790), *SlPDI7-2* (Solyc11g019920), *SlMC8* (Solyc10g081300), *SlWRKY1* (Solyc07g047960), *SlWRKY3* (Solyc08g081610), Solyc07g064820 (Mitogen-activated protein kinase kinase 2-like), Solyc07g040960 (Salt responsive protein 2) and *SlGPAT6* (Solyc09g014350) in the co-expression network of *SlHVA22g* [49–55]; *SlRabGAP9a* (Solyc07g049580), *SlRabGAP21a* (Solyc12g009610), *SlGT-33* (Solyc12g043090), *SlFdAT1* (Solyc12g088170), Solyc11g045120 (Translation initiation factor SUI1) and Solyc11g044910 (β-D-xylosidase) in that of *SlHVA22k* [56–62]; and Solyc10g078600 (phosphate transporter 1–1), *C2H2 zinc finger* (*C2H2-ZF*) (Solyc11g017140), Solyc11g045120 (Translation initiation factor SUI1), Solyc11g044910 (β-D-xylosidase), *SlRabGAP9b* (Solyc12g005930), *SlRabGAP21a* (Solyc12g009610) and *SlFdAT1* (Solyc12g088170) in that of *SlHVA22l* [56, 57, 59, 61, 63, 64] (Fig. 6 and Table S12). These findings suggested that these three genes, whose transcript levels were high in fruit and induced by abiotic stresses, likely function together with the co-expressed genes in the fruit development and abiotic stress response of tomato.

Conclusions

Plant *HVA22* genes respond to ABA and environmental cues to govern plant adaptation to abiotic stressors in cooperation with a variety of genes, including genes encoding stress-related transcription factors and ER resident proteins. We identified and comprehensively characterized 15 non-redundant *SlHVA22* genes residing on 8 of 12 tomato chromosomes. We postulate that tomato *HVA22* genes play roles in signaling cascades, development processes and abiotic stress responses of plants based on the following evidence: i) the prevalence of hormone- and abiotic stress–responsive *cis* elements, ii) the miRNA target sites and phosphorylation sites in their sequences, iii) their localization to the ER, iv) their predicted transporter activity and binding ability to diverse ligands, v) their co-expression with diverse genes involved in metabolic processes and vi) their differential expression patterns in various organs and under diverse abiotic stresses. The predominant expression of *SlHVA22i* in fruits at the breaker stage and 5 d after the breaker stage revealed that this gene may have an important regulatory role in fruit ripening. Many *SlHVA22* genes, including *SlHVA22b*, *SlHVA22i*, *SlHVA22k*, *SlHVA22l*, *SlHVA22m* and *SlHVA22n*, were markedly up- or downregulated on exposure to the stress hormone ABA and abiotic stressors, hinting that they might be actively involved in the abiotic stress tolerance of tomato through ABA-dependent pathways. Taken together, our results will be valuable for further investigation of the potential *SlHVA22* genes that may be exploited for the genetic improvement of tomato.

Methods

Genome-wide identification and sequence analysis of

SlHVA22 **genes**

The *SlHVA22* gene family members were identified form tomato genome by BLAST searches in the Sol Genomics database (http://solgenomics.net/) [65] using *Arabidopsis thaliana* HVA22 protein sequences retrieved from TAIR (https://www.Arabidopsis.org/) and HMM profile of SlHVA22 (PF03134) downloaded from Pfam prottein family database (http://pfam.xfam.org/) as a query. Subsequently, the NCBI CDD search (https://www.ncbi.nlm.nih.gov/Structure/bwrpsb/bwrpsb.cgi) and the SMART web tool (http://smart.emblheidelberg.de/) were used to confirm the presence of the TB2/DP1/HVA22 domain in the resulting fifteen non-redundant HVA22 protein sequences. The transmembrane domains (TMDs) in the SlHVA22 proteins were predicted through the web tool “TMHMM 2.0” (https://services.healthtech.dtu.dk/service.php?TMHMM-2.0) [66]. The ExPASy-ProtParam tool (http://cn.expasy.org/tools/protparam.html) was used to analyze the protein length, molecular weight, isoelectric point and GRAVY values (grand average of hydropathicity index) of each SlHVA22 protein [67]. The open reading frames of the *SlHVA22* genes were determined using the Open Reading Frame Finder tool (https://www.ncbi.nlm.nih.gov/orffinder/). The exon–intron distribution of *SlHVA22* genes was analyzed using the Gene Structure Display Server (GSDS) (http://gsds.cbi.pku.edu.cn/) [68]. A multi-protein sequence alignment was conducted using the Clustal Omega and ESPript web tools [69, 70]. The Multiple EM for Motif Elicitation (MEME) online tool (http://meme-suite.org/) was used to determine the conserved motifs in the full-length protein sequences with the following parameters: maximum number of motifs 10 and a motif length between six and 50 amino acids [71]. The web server “Immunomedicine Group” (http://imed.med.ucm.es/Tools/sias.html) was used to investigate the sequence homology of SlHVA22 proteins. The subcellular localizations of the tomato HVA22 proteins were predicted using WoLF-PSORT (https://wolfpsort.hgc.jp/) [72].

Phylogenetic analysis

The full-length HVA22 protein sequences were aligned with ClustalW and then the phylogenetic tree was built using the neighbor-joining (NJ) algorithm with 1000 bootstrap replications in MEGA 6.0 [73]. The deduced amino acid sequences used in the phylogenetic analysis were retrieved from the Phytozome and NCBI databases, except those of citrus obtained from the literature [6]. The names of the genes and their accession numbers used in the phylogenetic tree are described in Table S1.

Analysis of chromosomal localization, gene duplication and microsyntenic relationship

The chromosomal locations of the 15 tomato *HVA22* genes identified from the Sol genomic database were used to map the genes to their respective chromosomes with the online tool MapGene2Chrom web v2 (http://mg2c.iask.in/mg2c_v2.0/). The gene duplication events among *SlHVA22* genes were analyzed with the one-step MCScanX algorithm in the TBtools software [74] and examined by BLASTP with the E-value < 10^{-10}. The evolutionary constraint (Ka/ Ks) between the tomato duplicated gene pairs of genes were computed using the method of Nei and Gojobori (1986) [75]. The divergence time (T) of the duplicated gene pair was predicted using the formula T = Ks/2r Mya (millions of years), where r is the constant for dicotyledonous plants of 1.5×10^{-8} substitutions per site per year and Ks is the synonymous substitution rate per site [76]. The microsyntenic relationship of *HVA22* genes across Arabidopsis, tomato and rice was explored by performing a reciprocal BLAST search against their whole genomes, and the identified duplicated gene pairs were visualized with the TBtools software [74].

Prediction of phosphorylation sites, N-glycosylation sites, miRNA target sites, and cis**-regulatory elements**

The putative phosphorylation sites (Ser/Thr/Tyr), N-glycosylation sites (tipo Asn-X-Ser/Thr) and miRNA targets were predicted using the NetPhos 3.1 web-based tool [77], the NetNGlyc 1.0 server (http://www.cbs.dtu.dk/ services/NetNGlyc/), and the psRNATarget web tool (http://plantgrn.noble.org/psRNATarget/analysis), respectively. The promoter regions of 1500 bp upstream of the initiation codon [ATG] was analyzed to predict the putative *cis*-regulatory elements in SlHVA22 promoters through the PlantCare web server (http://bioinformatics.psb.ugent.be/webtools/plantcare/html/) [78].

3D model perdition of tomato SlHVA22 proteins

The comparative modelling of tomato SlHVA22 proteins were performed by the I-TASSER server using the amino acid sequences of SlHVA22a-o as input [24]. The prediction of 3-D models was conducted by multiple threading alignments with LOMETS and iterative structure assembly simulations. The template analogues were identified and the optimal models were chosen based on the highest scores. ModRefiner was used for the refinement of the obtaining modelled structures [79]. The final 3-dimensional models of SlHVA22 proteins were generated using Discovery Studio v.21.1. The putative functions of the resulting modelled proteins were estimated with the I-TASSER server based on global and local homology to template proteins curated in PDB with identified structures and functions.

Co-expression network analysis of SlHVA22 **genes**

Raw RNA-seq reads were downloaded from the SRA database (https://www.ncbi.nlm.nih.gov/sra) under the accessions SRR404309, SRR404310, SRR404311, SRR404312, SRR404313, SRR404314, SRR404315, SRR404316, SRR988278, SRR988418, SRR988529, SRR988530-SRR988532, SRR988533-SRR988535, SRR404317-SRR404322, and SRR404324-SRR404329. FastQC toolkit was used to assess raw sequence reads [80]. The raw reads were cleaned by removing low quality reads and trimming adaptor sequences from raw data. Then, the cleaned reads were mapped against tomato reference genome ITAG4.0 by using HISAT software and produced a non-redundant genome features annotation file (gff) [81]. Only reads uniquely mapped to the non-redundant gff annotated site were kept for expression analysis. The expression was calculated as the fragment per kb per million reads (FPKM) by using Cuffdiff software. For the co-expression genes with SlHVA22 genes, weighted gene co-expression network analysis (WGCNA) was performed with those genes having FPKM greater than 1 in R [82]. Cytoscape (https://cytoscape.org/) was used to construct the co-expression networks. The GO and KEGG annotations of co-expressed genes with were conducted by PANTHER and Kyoto Encyclopedia of Genes and Genomes (KEGG) Server (http://www.genome.jp/kegg/kaas/), respectively.

Subcellular localization analyses

The full-length coding sequences of *SlHVA22* genes were first amplified using the gene-specific primers (Table S2). Then, they were cloned in the pGA3452 vector to express SlHVA22-GFP fusion proteins under the control of the maize *Ubi1* promoter [83]. NLS-mRFP driven by the 35S promoter served as a nuclear marker. The SlHVA22-GFP fusion construct and NLS-mRFP construct were co-transfected into the protoplasts prepared from rice Oc cells through electroporation method [84]. After the transfected protoplasts were incubated at 28°C in the dark for 12 to 16 h, the localization of the fusion protein was determined using a confocal fluorescence microscope (BX61; Olympus, Tokyo, Japan).

Preparation of plant materials and stress treatments

Plant materials (seeds of *Solanum lycopersicum* cv Ailsa Craig) were obtained from the Giovannoni laboratory at the Boyce Thompson Institute. Tomato plants were grown in soil in the growth chamber maintained at an adjusted temperature of 25°C day/20°C night, a 16 h light/8 h dark photoperiod, a relative humidity of 55 to 70%, and a light intensity of 300 μmol $m^{-2}s^{-1}$. For organ-specific expression profiling of *SlHVA22* genes, root, stem, and leaf tissues were harvested from 28-day-old plants. The remaining plants were transferred to a greenhouse adjusted at a temperature of 25°C/day and 20°C /night and 65–80% relative humidity for sampling of flowers and fruits at the reproductive stage. Fresh fruits were collected at five different developmental stages: (i) young fruits approximately 7 days after the date of pollination and 1 cm in diameter (1 cm fruits); (ii) immature fruits approximately 21 days after the date of pollination (IM fruits); (iii) mature green fruits approximately 35 days after the date of pollination (MG fruits); (iv) fruits at the breaker stage when the color of mature fruits turns to light yellow-orange from green (B fruits); and (v) fruits 5 days after the breaker stage (B5 fruits).

Leaf samples from 28-day-old plants with synchronized growth were harvested at 0, 24, 48, 60, and 72 h after the start of the drought treatment and at 0, 1, 3, 9, and 24 h after the start of other abiotic stress treatments, such as cold, heat, salt [NaCl], and abscisic acid [ABA] to examine the expression profiles of *SlHVA22* genes upon exposure to various abiotic stressors. Drought treatment was subjected to the plants by withholding watering for 72h. The measurement of relative water content (RWC) was conducted in three biological replications using the mature fully expanded leaflet at 0, 24, 48, 60 and 72 h after the drought treatment as described by Collin et al. (2020) (Fig. S8) [85]. ABA treatment was imposed by spraying the leaves of tomato plants with 100 μM ABA solution. To apply the cold and heat stresses, the tomato plants were incubated in the growth cabinet maintained at 4°C and 40°C for 24 h, respectively. For salt treatment, tomato plants were transferred to nutrient solution with 200 mM NaCl and the plants in the nutrient solution is used as the 0 h control [86]. Plants grown in soil under normal conditions (25°C) were used as the 0 h controls for ABA, heat, cold and drought treatment. All samples were collected from three biological replicates, immediately frozen in liquid nitrogen, and stored at − 80°C for RNA isolation and cDNA synthesis.

RNA extraction and quantitative RT-PCR analysis

Total RNA was extracted from the plant samples with an RNeasy Mini kit (Qiagen, Hilden, Germany) and purified using an RNase-free DNase I kit (Qiagen, Hilden, Germany) as per manufacturer's instructions. A NanoDrop® 1000 spectrophotometer (Wilmington, DE, USA) was used to measure the quantity and quality of the extracted RNA. cDNA synthesis was performed using 1 μg total RNA with a Superscript® III First-Strand cDNA synthesis kit (Invitrogen, Carlsbad, CA, USA). The gene-specific primers for all tomato *HVA22* genes were designed using Primer3 software (http://frodo.wi.mit.edu/primer3/input.htm) (Table S3). The specificity of the amplicons for the primer pairs used in the expression analysis was validated by melting curve analysis [87]. The primer for *Le18S rRNA* (F: AAAAGGTCGACGCGGGCT, R: CGACAGAAGGGACGAGAC) was used as a reference gene for normalization [88]. The reaction mixture for qRT-PCR analysis was composed of 1 μL (50 ng) cDNA, 2 μL forward and reverse primers (5 pmol concentration), 2 μL double distilled water, and 5 μL of iTaq SYBR Green (Qiagen, Hilden, Germany). A Light cycler® 96SW 1.1 instrument (Roche, Germany) was used for amplification and determination of the Cq value of each sample with the following parameters: pre-denaturation at 95°C for 5 min

followed by 40 cycles of 95°C for 15 s, annealing at 58°C for 20 s, and extension at 72°C for 40 s. The $2^{-\Delta\Delta Ct}$ method was used to analyse the relative expression of each gene against each treatment [89].

Statistical analysis

The statistical analysis of the data was performed with SigmaPlot 14 (SYSTAT and MYSTAT Products, United States, and Canada) using two-tailed Student's t-tests. *P < 0.05, **P < 0.01 and ***P < 0.001 were considered statistically significant.

Abbreviations

TB2/Dp1: deleted in polyposis 1; ER: Endoplasmic reticulum; TMD: transmembrane domain; 3D: Three Dimensional; GFP: Green fluorescent protein; TM: Template modeling; RMSD: root-mean-square deviation; C-score: confident score; ABA: Abscisic acid; WGCNA: Weighted gene co-expression network analysis

Declarations

Ethics approval and consent to participate

Not Applicable.

Consent for publication

Not applicable.

Availability of data and materials

We declare that the dataset(s) required to reproduce the results of this article are included in the article and additional file(s) available in journal webpage.

Competing interests

The authors declare that they have no competing interests.

Funding

This work was financially supported from the National Research Foundation of Korea (NRF) Grant funded by the Korean government (MSIT) (no. NRF-2018R1A2B6001781).

Author Contributions

M-YC, D-JL, STK and C-KK designed the experiments. AHW and L-HC performed the experiments. AHW and MW conducted the in silico analysis. AHW analyzed the data. AHW wrote the manuscript. All authors approved the article.

Acknowledgements

Not applicable.

References

1. Guo WJ, David Ho TH. An abscisic acid-induced protein, HVA22, inhibits gibberellin-mediated programmed cell death in cereal aleurone cells. Plant physiol. 2008;147:1710-22.
2. Sharon K, Suvarna S. Cloning of HVA22 homolog from Aloe vera and preliminary study of transgenic plant development. Int. J. Pure App. Biosci, 2017;5:1113-21.
3. Shen Q, Chen CN, Brands A, Pan SM, Ho TH. The stress- and abscisic acid induced barley gene HVA22: developmental regulation and homologues in diverse organisms. Plant Mol. Biol. 2001;45:327-340. doi:
4. Shen Q, Uknes SJ, Ho TD. Hormone response complex in a novel abscisic acid and cycloheximide-inducible barley gene. J. Biol. Chem. 1993;268:23652-60.
5. Brands A,Ho THD. Function of a plant stress-induced gene, HVA22. Synthetic enhancement screen with its yeast homolog reveals its role in vesicular traffic. Plant physiol. 2002;130: 1121-31.
6. Ferreira MDG, Castro JA, Silva RJS, Micheli F. HVA22 from citrus: a small gene family whose some members are involved in plant response to abiotic stress. Plant Physiol Biochem. 2019;142:395-404.
7. Hu J, Shibata Y, Voss C, Shemesh T, Li Z, Coughlin M, Kozlov MM, Rapoport TA, Prinz WA. Membrane proteins of the Endoplasmic reticulum induce high-curvature tubules. Science. 2008;319:1247-50.

8. Voeltz GK, Prinz WA, Shibata Y, Rist JM, Rapoport TA. A class of membrane proteins shaping the tubular endoplasmic reticulum. Cell. 2006;124:573-86.
9. Shen Q, Ho THD. Functional dissection of an abscisic acid (ABA)-inducible gene reveals two independent ABA-responsive complexes each containing a G-box and a novel cis-acting element. Plant Cell. 1995;7:295-307.
10. Shen Q, Ho THD. Promoter switches specific for abscisic acid (ABA)-induced gene expression in cereals. Physiol. Plant. 1997;101:653-64.
11. Su J, Shen Q, David Ho TH, Wu R. Dehydration-stress-regulated transgene expression in stably transformed rice plants. Plant Physiol. 1998;117:913-922.
12. Casaretto J, Ho THD. The transcription factors HvABI5 and HvVP1 are required for the abscisic acid induction of gene expression in barley aleurone cells. Plant Cell. 2003;15:271-84.
13. Niu X, Helentjaris T, Bate NJ. Maize ABI4 binds coupling element1 in abscisic acid and sugar response genes. Plant Cell. 2002;14:2565-75.
14. Zhang ZL, Shin M, Zou X, Huang J, Ho THD, Shen QJ. A negative regulator encoded by a rice WRKY gene represses both abscisic acid and gibberellins signaling in aleurone cells. Plant Mol Biol.2009;70:139-51.
15. Zou X, Seemann JR, Neuman D, Shen QJ. A WRKY gene from creosote bush encodes an activator of the abscisic acid signaling pathway. J Biol Chem. 2004;279:55770-9.
16. Wai AH, Naing AH, Lee DJ, Kim CK, Chung MY. Molecular genetic approaches for enhancing stress tolerance and fruit quality of tomato. Plant Biotechnol Rep. 2020:1-23.
17. Chen CN, Chu CC, Zentella R, Pan SM, David Ho TH. *AtHVA22* gene family in Arabidopsis: phylogenetic relationship, ABA and stress regulation, and tissue-specific expression. Plant Mol Biol. 2002;49:631-42.
18. Courtney AJ, Xu J, Xu Y. Responses of growth, antioxidants and gene expression in smooth cordgrass (*Spartina alterniflora*) to various levels of salinity. Plant Physiol. Biochem. 2016;99:162-70.
19. Xiao BZ, Chen X, Xiang CB, Tang N, Zhang QF, Xiong LZ. Evaluation of seven function-known candidate genes for their effects on improving drought resistance of transgenic rice under field conditions. Mol Plant. 2009;2:73-83.
20. Hu N, Tang N, Yan F, Bouzayen M, Li Z. Effect of LeERF1 and LeERF2 overexpression in the response to salinity of young tomato (*Solanum lycopersicum* cv. Micro-Tom) seedlings. Acta Physiol. Plant. 2014;36:1703-12.
21. Verma V, Ravindran P, Kumar PP. Plant hormone-mediated regulation of stress responses. BMC Plant Biol. 2016;16:1-10.
22. Filipowicz W, Bhattacharyya SN, Sonenberg N. Mechanisms of post-transcriptional regulation by microRNAs: are the answers in sight? Nat rev genet. 2008;9:102-14.
23. López-Galiano MJ, Sentandreu V, Martínez-Ramírez AC, Rausell C, Real MD, Camañes G, Ruiz-Rivero O, Crespo-Salvador O, García-Robles I. Identification of stress associated microRNAs in Solanum lycopersicum by high-throughput sequencing. Genes. 2019;10:475.
24. Yang J, Yan R, Roy A, Xu D, Poisson J, Zhang Y. The I-TASSER Suite: protein structure and function prediction. Nat. Methods. 2015;12:7-8.
25. Merchant SS, Prochnik SE, Vallon O, Harris EH, Karpowicz SJ, Witman GB, Terry A, Salamov A, Fritz-Laylin LK, Maréchal-Drouard L, Marshall WF. The Chlamydomonas genome reveals the evolution of key animal and plant functions. Science. 2007;318:245-50.
26. Wolfe KH, Gouy M, Yang YW, Sharp PM, Li WH. Date of the monocot-dicot divergence estimated from chloroplast DNA sequence data. Proc Natl Acad Sci. 1989;86:6201-5.
27. Biłas R, Szafran K, Hnatuszko-Konka, K. Kononowicz AK. Cis-regulatory elements used to control gene expression in plants. Plant Cell Tiss Organ Cult. 2016;127:269-87.
28. Priest HD, Filichkin SA, Mockler TC. Cis-regulatory elements in plant cell signaling. Curr Opin Plant Biol. 2009;12:643-9.
29. Çakır Ö, Arıkan B, Karpuz B, Turgut-Kara N. Expression analysis of miRNAs and their targets related to salt stress in *Solanum lycopersicum* H-2274. Biotechnol. Biotechnol. Equip. 2021;35: 283-90.
30. Liu M, Yu H, Zhao G, Huang Q, Lu Y, Ouyang B. Profiling of drought-responsive microRNA and mRNA in tomato using high-throughput sequencing. BMC Genomics. 2017;18: 481.
31. Liu M, Yu H, Zhao G, Huang Q, Lu Y, Ouyang B. Identification of drought-responsive microRNAs in tomato using high-throughput sequencing. Funct Integr Genomics. 2018;18: 67-78.
32. Wang Z, Li N, Yu Q, Wang H. Genome-Wide Characterization of Salt-Responsive miRNAs, circRNAs and Associated ceRNA Networks in Tomatoes. Int J Mol Sci., 2021;22:12238.
33. Ardito F, Giuliani M, Perrone D, Troiano G, Lo Muzio L. The crucial role of protein phosphorylation in cell signaling and its use as targeted therapy. Int J Mol Med. 2017;40: 271-80.
34. Hashiguchi A, Komatsu S. Impact of post-translational modifications of crop proteins under abiotic stress. Proteomes. 2016;4:42.
35. Giovannoni JJ. Genetic regulation of fruit development and ripening. Plant Cell. 2004 ;16:170-80.
36. Giovannoni JJ. Fruit ripening mutants yield insights into ripening control. Curr Opin Plant Biol. 2007;10:283-9.
37. Lemaire-Chamley M, Petit J, Garcia V, Just D, Baldet P, Germain V, Fagard M, Mouassite M, Cheniclet C, Rothan C: Changes in transcriptional profiles are associated with early fruit tissue specialization in tomato. Plant Physiol. 2005;139:750-9.

38. Banerjee A, Roychoudhury A. Abscisic-acid-dependent basic leucine zipper (bZIP) transcription factors in plant abiotic stress. Protoplasma. 2017;254:3-16.
39. Hernández Y, Sanan-Mishra N. miRNA mediated regulation of NAC transcription factors in plant development and environment stress response. Plant Gene.2017;11:190-8.
40. Qin F, Shinozaki K, Yamaguchi-Shinozaki K. Achievements and challenges in understanding plant abiotic stress responses and tolerance. Plant Cell Physiol. 2011;52:1569-82.
41. Saibo NJ, Lourenço T, Oliveira MM. Transcription factors and regulation of photosynthetic and related metabolism under environmental stresses. Ann Bot. 2009;103:609-23.
42. Huang YC, Niu CY, Yang CR,Jinn, TL. The heat stress factor HSFA6b connects ABA signaling and ABA-mediated heat responses. Plant Physiol. 2016;172:1182-99.
43. Luo DL, Ba LJ, Shan W, Kuang JF, Lu WJ, Chen JY. Involvement of WRKY transcription factors in abscisic-acid-induced cold tolerance of banana fruit. J agric food chem.2017;65:3627-35.
44. Suzuki N, Bassil E, Hamilton JS, Inupakutika MA, Zandalinas SI, Tripathy D, et al. ABA is required for plant acclimation to a combination of salt and heat stress. PLoS One. 2016;11:e147625.
45. Cai J, Meng X, Li G, Dong T, Sun J, Xu T, Li Z, Han Y, Zhu M. Identification, expression analysis, and function evaluation of 42 tomato DEAD-box RNA helicase genes in growth development and stress response. Acta Physiol Plant. 2018;40:94.
46. Xu R, Zhang S, Lu L, Cao H, Zheng C. A genome-wide analysis of the RNA helicase gene family in Solanum lycopersicum. Gene. 2013;513:128-40.
47. Yang X, Zhu W, Zhang H, Liu N, Tian S. Heat shock factors in tomatoes: genome-wide identification, phylogenetic analysis and expression profiling under development and heat stress. PeerJ. 2016;4:e1961.
48. Jia J, Liang Y, Gou T, Hu Y, Zhu Y, Huo H, Guo J, Gong, H. The expression response of plasma membrane aquaporins to salt stress in tomato plants. Environ. Exp. Bot. 2020;178:104190.
49. Duan Y, Yang L, Zhu H, Zhou J, Sun H, Gong H. Structure and expression analysis of sucrose phosphate synthase, sucrose synthase and invertase gene families in *Solanum lycopersicum*. Int J Mol Sci. 2021;22: 4698.
50. Karkute SG, Gujjar RS, Rai A, Akhtar M, Singh M, Singh B. Genome wide expression analysis of WRKY genes in tomato (*Solanum lycopersicum*) under drought stress. Plant Gene. 2018;13:8-17.
51. Liu H, Liu J, Wei Y. Identification and analysis of the metacaspase gene family in tomato. Biochem Biophys Res Commun. 2016;479:523-9.
52. Liu H, Zhou Y, Li H, Wang T, Zhang J, Ouyang B, Ye Z. Molecular and functional characterization of ShNAC1, an NAC transcription factor from Solanum habrochaites. Plant Sci. 2018;271:9-19.
53. Meng X, Cai J, Deng L, Li G, Sun J, Han Y, Dong T, Liu Y, Xu T, Liu S, Li Z. SlSTE1 promotes abscisic acid-dependent salt stress-responsive pathways via improving ion homeostasis and reactive oxygen species scavenging in tomato. J Integr Plant Biol. 2020;62: 1942-66.
54. Petit J, Bres C, Mauxion JP, Tai FWJ, Martin LB, Fich EA, Joubès J, Rose JK, Domergue F, Rothan C. The glycerol-3-phosphate acyltransferase GPAT6 from tomato plays a central role in fruit cutin biosynthesis. Plant Physiol. 2016;171:894-913.
55. Wai AH, Waseem M, Khan AB, Nath UK, Lee DJ, Kim ST, Kim CK, Chung MY. Genome-Wide Identification and Expression Profiling of the PDI Gene Family Reveals Their Probable Involvement in Abiotic Stress Tolerance in Tomato (*Solanum lycopersicum* L.). Genes. 2021;12:23.
56. Bemer M, Karlova R, Ballester AR, Tikunov YM, Bovy AG, Wolters-Arts M, Rossetto PB, Angenent GC, Maagd RA: The tomato FRUITFULL homologs TDR4/FUL1 and MBP7/FUL2 regulate ethylene-independent aspects of fruit ripening. Plant Cell. 2012;24: 4437-51.
57. Jian W, Cao H, Yuan S, Liu Y, Lu J, Lu W, Li, N., Wang J, Zou J, Tang N, Xu C. SlMYB75, an MYB-type transcription factor, promotes anthocyanin accumulation and enhances volatile aroma production in tomato fruits. Hortic Res. 2019;6:22.
58. Madrid-Espinoza J, Salinas-Cornejo J, Ruiz-Lara S. The RabGAP gene family in tomato (*Solanum lycopersicum*) and wild relatives: identification, interaction networks, and transcriptional analysis during plant development and in response to salt stress. Genes. 2019;10:638.
59. Morcillo RJ, Vílchez JI, Zhang S, Kaushal R, He D, Zi H, Liu R, Niehaus K, Handa AK, Zhang H. Plant transcriptome reprograming and bacterial extracellular metabolites underlying tomato drought resistance triggered by a beneficial soil bacteria. Metabolites. 2021;11:369.
60. Olivieri F, Calafiore R, Francesca S, Schettini C, Chiaiese P, Rigano MM, Barone A. High-throughput genotyping of resilient tomato landraces to detect candidate genes involved in the response to high temperatures. Genes. 2020;11:626.
61. Shukla V, Fatima T, Goyal RK, Handa AK, Mattoo AK. Engineered ripening-specific accumulation of polyamines spermidine and spermine in tomato fruit upregulates clustered C/D box snoRNA gene transcripts in concert with ribosomal RNA biogenesis in the red ripe fruit. Plants.2020; 9:1710.
62. Yu C, Cai X, Ye Z, Li H. Genome-wide identification and expression profiling analysis of trihelix gene family in tomato. Biochem Biophys Res Commun. 2015;468:653-9.
63. Hu X, Zhu L, Zhang Y, Xu L, Li N, Zhang X, Pan Y. Genome-wide identification of C2H2 zinc-finger genes and their expression patterns under heat stress in tomato (*Solanum lycopersicum* L.). PeerJ. 2019;7:e7929.
64. Tian P, Lin Z, Lin D, Dong S, Huang J, Huang, T. The pattern of DNA methylation alteration, and its association with the changes of gene expression and alternative splicing during phosphate starvation in tomato. Plant J. 2021;108:841-58.
65. Mueller LA, Solow TH, Taylor N, Skwarecki B, Buels R, Binns J, Lin C, Wright MH, Ahrens R, Wang Y, Herbst EV. The SOL Genomics Network. A comparative resource for Solanaceae biology and beyond. Plant Physiol. 2005;138:1310-7.

66. Moller S, Croning MDR. Apweiler, R. Evaluation of methods for the prediction of membrane-spanning regions. Bioinformatics. 2001;17: 646–53.
67. Gasteiger E, Hoogland C, Gattiker A, Wilkins MR, Appel RD, Bairoch A. Protein identification and analysis tools on the ExPASy server. The proteomics protocols handbook. 2005:571-607.
68. Guo AY, Zhu QH, Chen X, Luo JC. GSDS: a gene structure display server. Yi Chuan. 2007;29:1023-6.
69. Robert X, Gouet P. Deciphering key features in protein structures with the new ENDscript server. Nucl Acids Res. 2014;42:320-4.
70. Sievers F, Wilm A, Dineen D, Gibson TJ, Karplus K, Li W, Lopez R, McWilliam H, Remmert M, Söding J, Thompson JD. Fast, scalable generation of high-quality protein multiple sequence alignments using Clustal Omega. Mol. Syst. Biol. 2011;7:539.
71. Bailey TL, Boden M, Buske FA, Frith M, Grant CE, Clementi L, Ren J, Li WW, Noble WS. MEME SUITE: tools for motif discovery and searching. Nucl Acids Res. 2009;37:202-8.
72. Horton P, Park KJ, Obayashi T, Fujita N, Harada H, Adams-Collier CJ, Nakai K. WoLF PSORT: protein localization predictor. Nucl Acids Res.. 2007;35:585-7.
73. Tamura K, Stecher G, Peterson D, Filipski A, Kumar S. MEGA6: molecular evolutionary genetics analysis version 6.0. Mol. Biol. Evol. 2013;30:2725-9.
74. Chen C, Chen H, Zhang Y, Thomas HR, Frank MH, He Y, Xia R. TBtools: an integrative toolkit developed for interactive analyses of big biological data. Mol. Plant. 2020;13:1194-202.
75. Nei M, Gojobori T. Simple methods for estimating the numbers of synonymous and nonsynonymous nucleotide substitutions. Mol Biol Evol. 1986;3:418-26.
76. Koch MA, Haubold B, Mitchell-Olds T. Comparative evolutionary analysis of chalcone synthase and alcohol dehydrogenase loci in Arabidopsis, Arabis, and related genera (Brassicaceae). Mol Biol Evol. 2000;17:1483-98.
77. Blom N, Gammeltoft S, Brunak S. Sequence- and structure-based prediction of eukaryotic protein phosphorylation sites. J. Mol. Biol. 1999;294:1351-62.
78. Lescot M, Déhais P, Thijs G, Marchal K, Moreau Y, Van de Peer Y, Rouzé P, Rombauts S. PlantCARE, a database of plant cis-acting regulatory elements and a portal to tools for *in silico* analysis of promoter sequences. Nucleic Acids Res. 2002;30:325-7.
79. Xu D, Zhang Y. Improving the physical realism and structural accuracy of protein models by a two-step atomic-level energy minimization. Biophys J. 2011;101:2525-34
80. Andrews S. FastQC: a quality control tool for high throughput sequence data. Babraham Bioinformatics, Babraham Institute, Cambridge, United Kingdom. 2010.
81. Kim D, Paggi JM, Park C, Bennett C, Salzberg SL. Graph-based genome alignment and genotyping with HISAT2 and HISAT-genotype. Nat biotechnol. 2019;37:907-15.
82. Langfelder P, Horvath S. WGCNA: an R package for weighted correlation network analysis. BMC bioinformatics. 2008;9:1-3.
83. Kim SR, Lee DY, Yang JI, Moon S, An G. Cloning vectors for rice. Journal of Plant Biology. 2009;52:73.
84. Page MT, Parry MA, Carmo-Silva E. A high-throughput transient expression system for rice. Plant Cell Environ. 2019;42. 2057-64.
85. Collin A, Daszkowska-Golec A, Kurowska M, Szarejko I. Barley ABI5 (Abscisic Acid INSENSITIVE 5) is involved in abscisic acid-dependent drought response. Front. Plant Sci. 2020;11:1138.
86. Wai, AH, Cho LH, Peng X, Waseem M, Lee DJ, Lee JM, Kim CK, Chung MY. Genome-wide identification and expression profiling of *Alba* gene family members in response to abiotic stress in tomato (*Solanum lycopersicum* L.). BMC Plant Biol. 2021;21:1–21.
87. Verma JK, Wardhan V, Singh D, Chakraborty S, Chakraborty N. Genome-wide identification of the *Alba* gene family in plants and stress-responsive expression of the rice *Alba* genes. Genes. 2018;9:183.
88. Balestrini R, Gómez-Ariza J, Lanfranco L, Bonfante P. Laser microdissection reveals that transcripts for five plant and one fungal phosphate transporter genes are contemporaneously present in arbusculated cells. Mol. Plant Microbe Interact. 2007;20:1055-62.
89. Schmittgen TD, Livak KJ. Analyzing real-time PCR data by the comparative CT method. Nat. Protoc. 2008;3:1101-8.

Figures

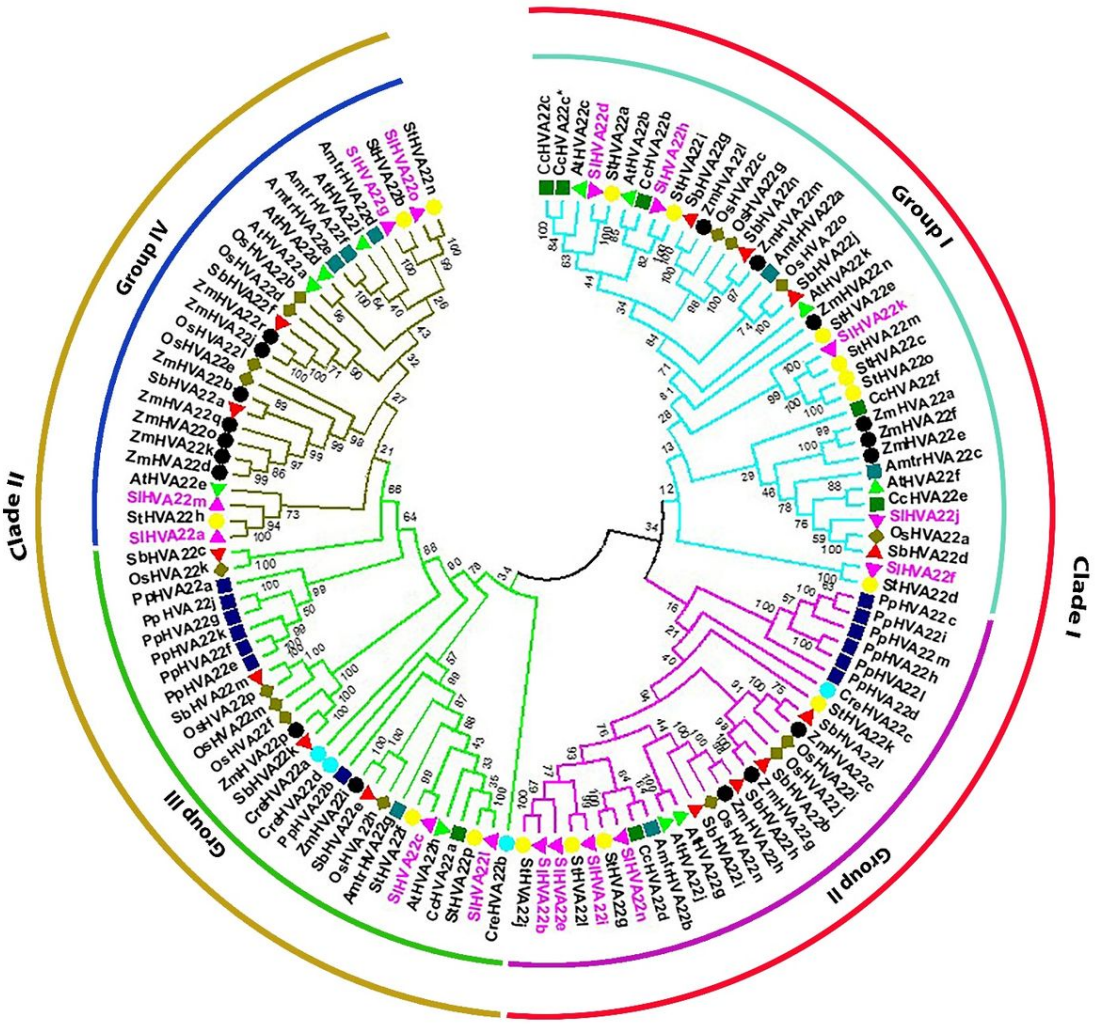

Figure 1

Phylogenetic analysis of HVA22 proteins from tomato and different plant species. The neighbor-joining tree was constructed with the full length HVA22 proteins using ClustalW and MEGA6 with 1000 bootstrap replicates. A species abbreviation was provided prior to each HVA22 protein name: Sl, *Solanum lycopersicum*; St, *Solanum tuberosum;* At, *Arabidopsis thaliana;* Os, *Oryza sativa*; Zm, *Zea mays*; Sb, *Sorghum bicolor*, Amtr, *Amborella trichopoda;* Pp, *Physcomitrella patens* and *Cre, Chlamydomonas reinhardtii.*

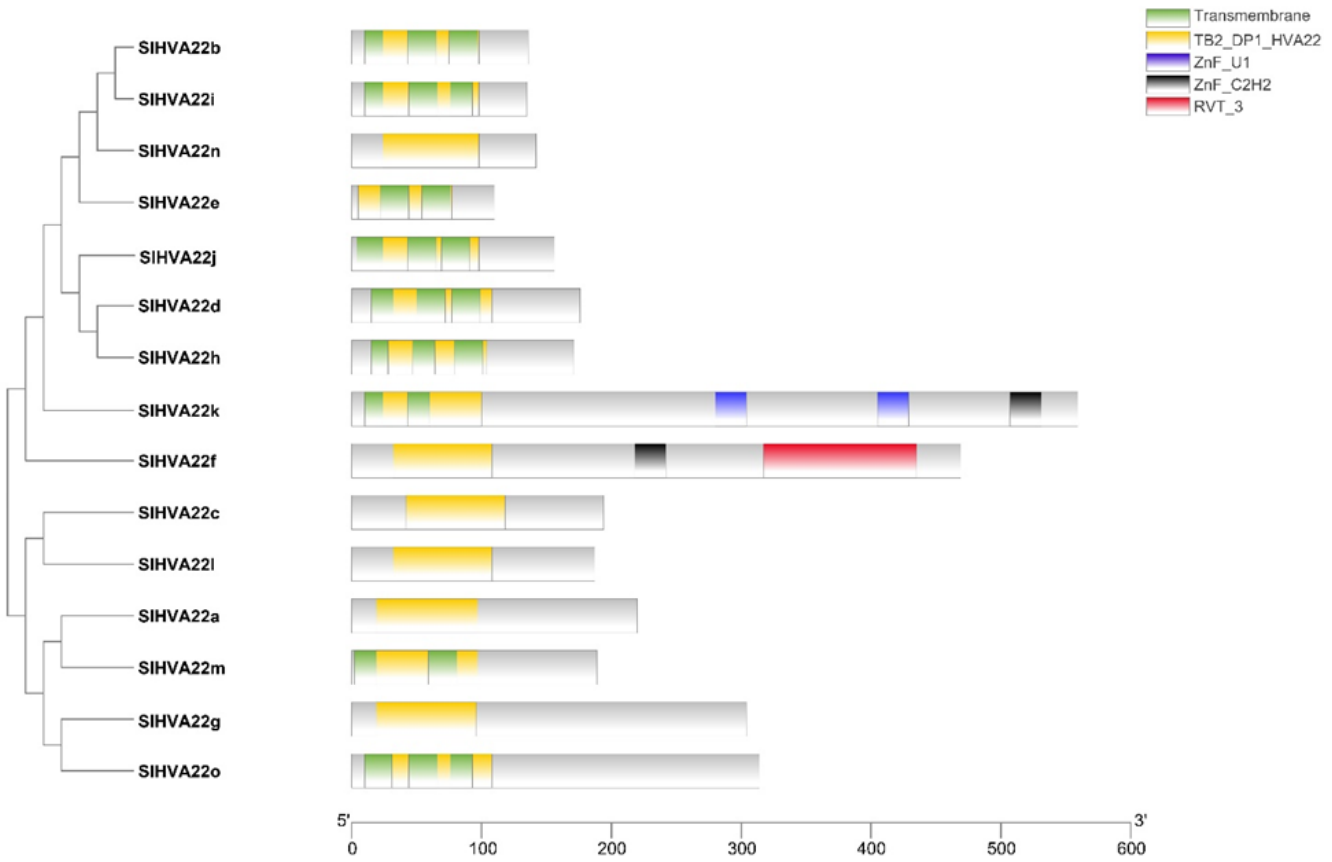

Figure 2

Schematic depiction of the domain organization of SlHVA22 proteins. The transmembrane domain, TB2/DP1/HVA22 domain, U1-type zinc finger (ZnF_U1) domain, the classical C2H2 zinc finger (ZnF_C2H2) domain and RVT_3 domain identified in SlHVA22 proteins are shown.

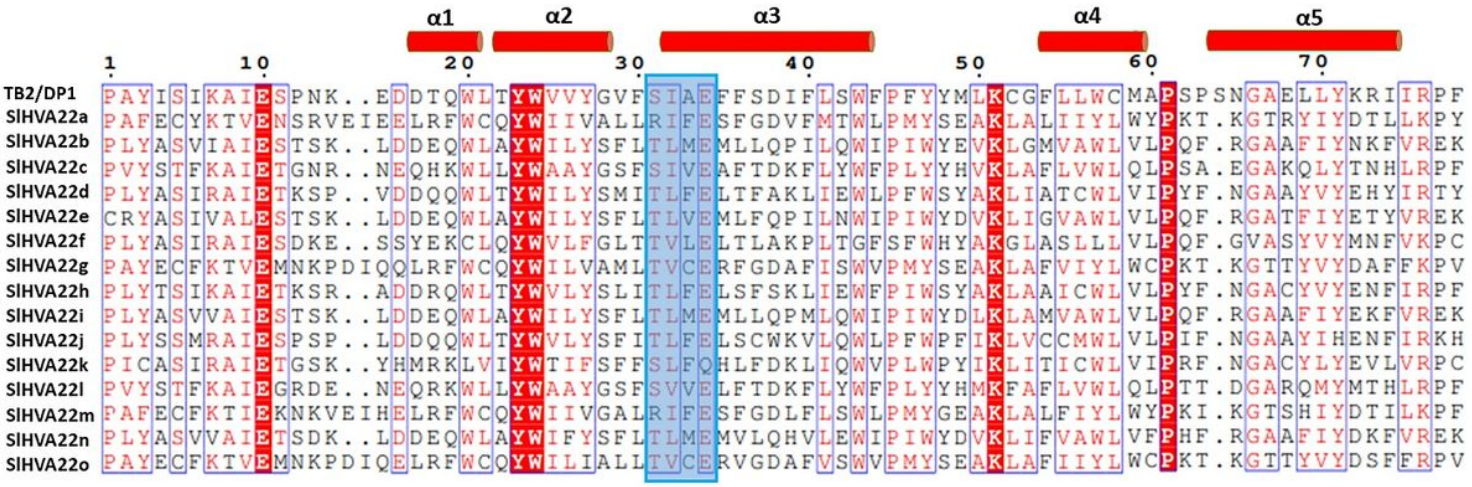

Figure 3

Alignment of TB2/DP1/HVA22 domains of SlHVA22 proteins with that of the typical human TB2/DP1. The secondary structural elements determined by the ESPript 3.0 web tool are indicated above the alignment. The putative conserved casein kinase II sites in the α-helix of TB2/DP1/HVA22 domain is marked by blue box.

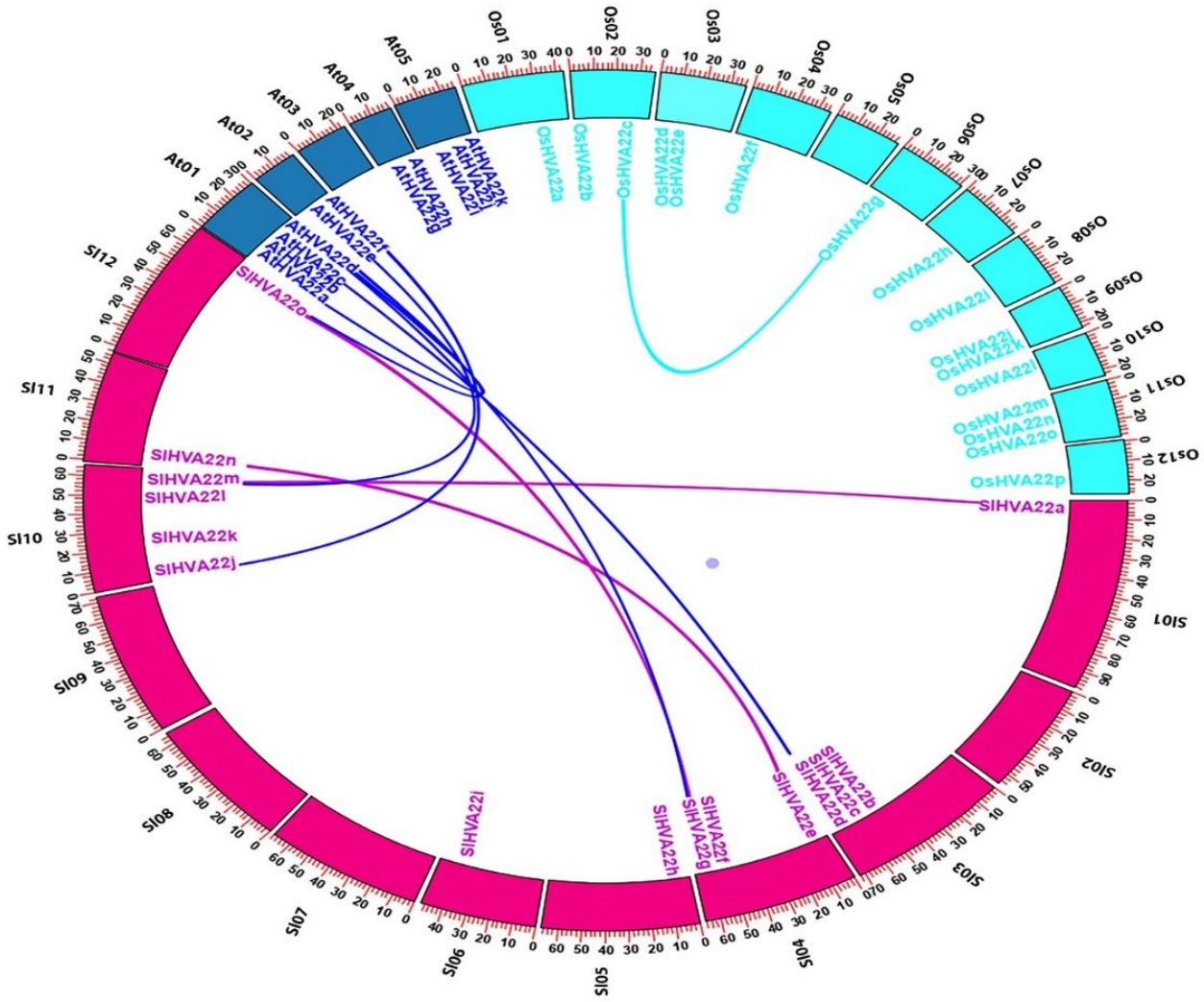

Figure 4

Microsyntenic relationship of *HVA22* genes across Arabidopsis, tomato, and rice. The chromosomes of the three species are depicted by different colors: Arabidopsis, blue; tomato, pink red; and rice, aqua. All chromosomes are illustrated with the scale in megabase pairs (Mbp). The duplicated *SlHVA22* genes in tomato genome are linked by pink red lines.

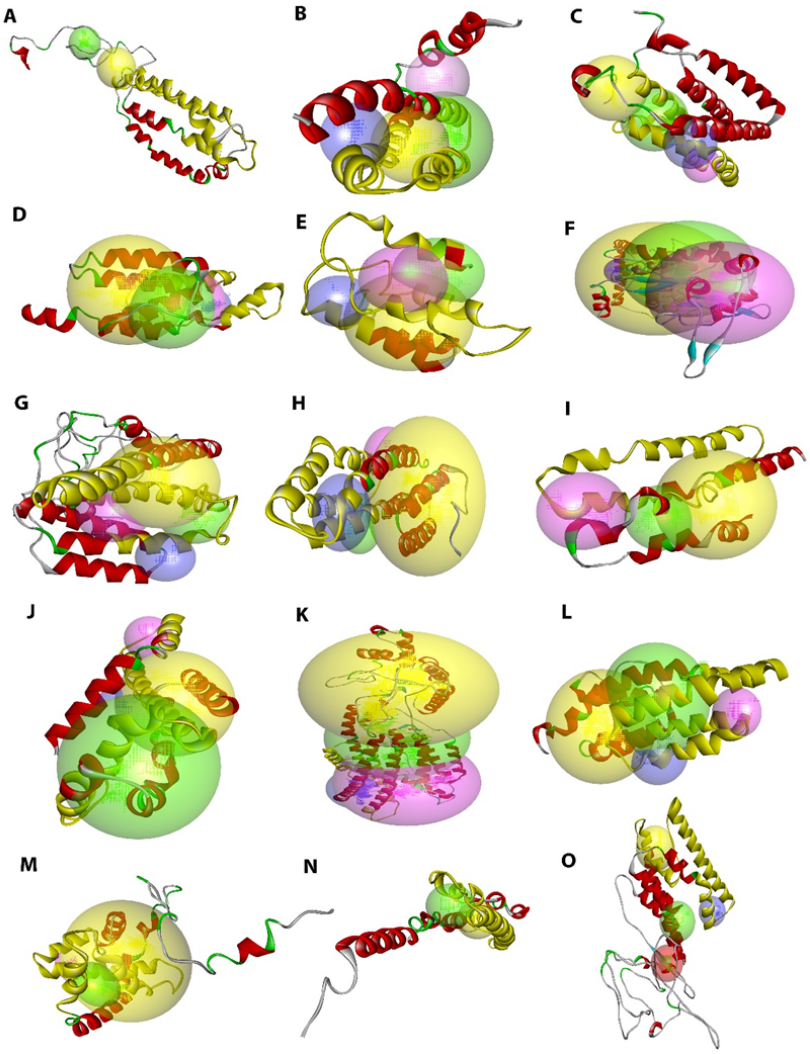

Figure 5

Predicted three-dimensional homology structure of tomato HVA22 proteins. The final 3D structures of SlHVA22 proteins were built by Discovery Studio v.21.1. The secondary structural components: α-helices (red), β-sheets (cyan), coils (green), and loops (gray) as well as the top four putative binding sites: site 1 (yellow sphere), site 2 (green sphere), site 3 (red sphere), and site 4 (blue sphere) are indicated in the predicted 3D models of (A) SlHVA22a; (B) SlHVA22b; (C) SlHVA22c; (D) SlHVA22d; (E) SlHVA22e; (F) SlHVA22f; (G) SlHVA22g; (H) SlHVA22h; (I) SlHVA22i; (J) SlHVA22j; (K) SlHVA22k; (L) SlHVA22l; (M) SlHVA22m; (N) SlHVA22n; and (O) SlHVA22o. TB2/DP1/HVA22 domain portions in the generated models are underlined in yellow.

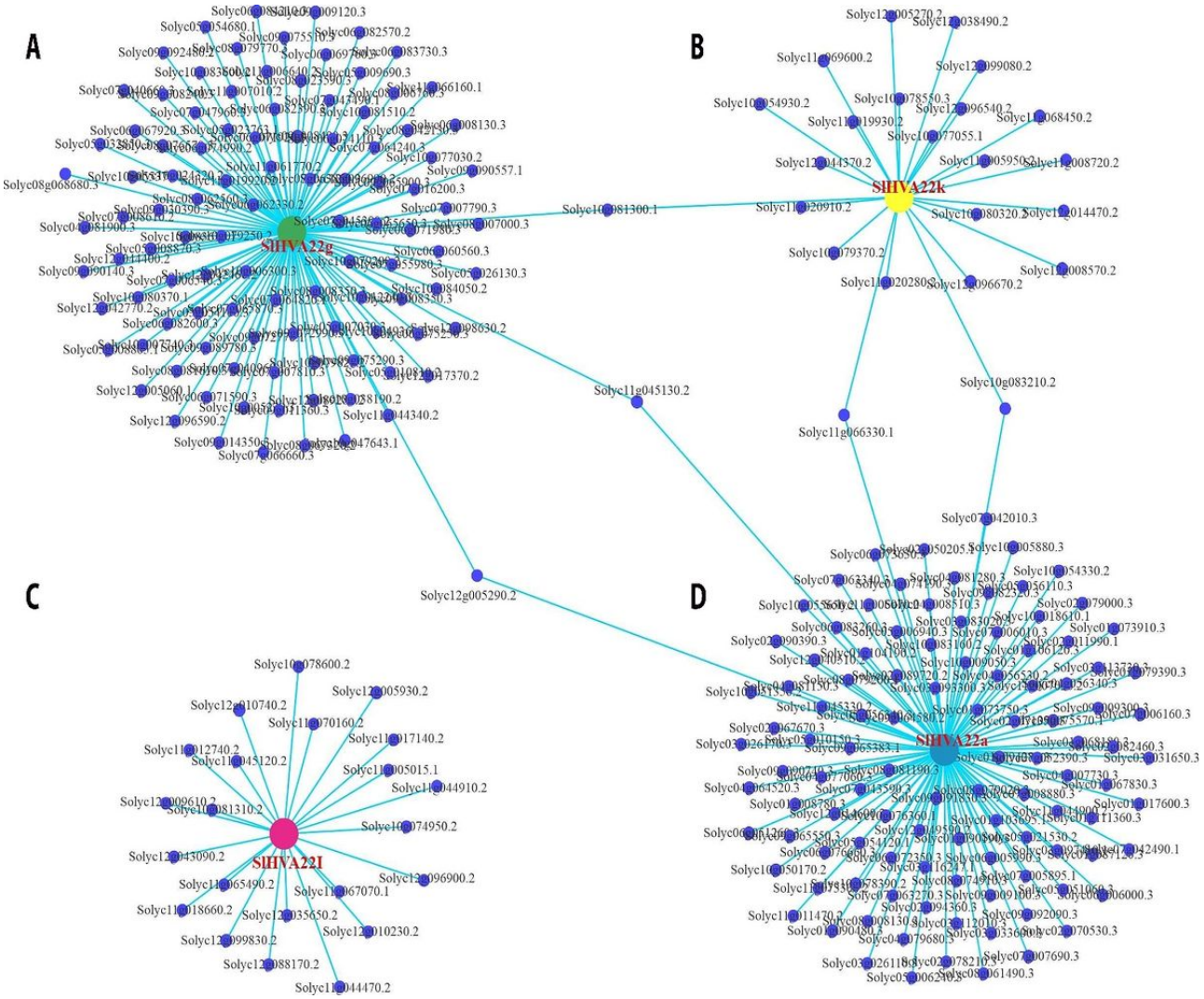

Figure 6

Weighted gene co-expression network analysis (WGCNA) of *SlHVA22* genes. A-D: The co-expressed genes in the network of *SHVA22g* (A), *SHVA22k* (B), *SlHVA22l*(C) and *SlHVA22a* (D). The *SlHVA22* genes are marked in red colour.

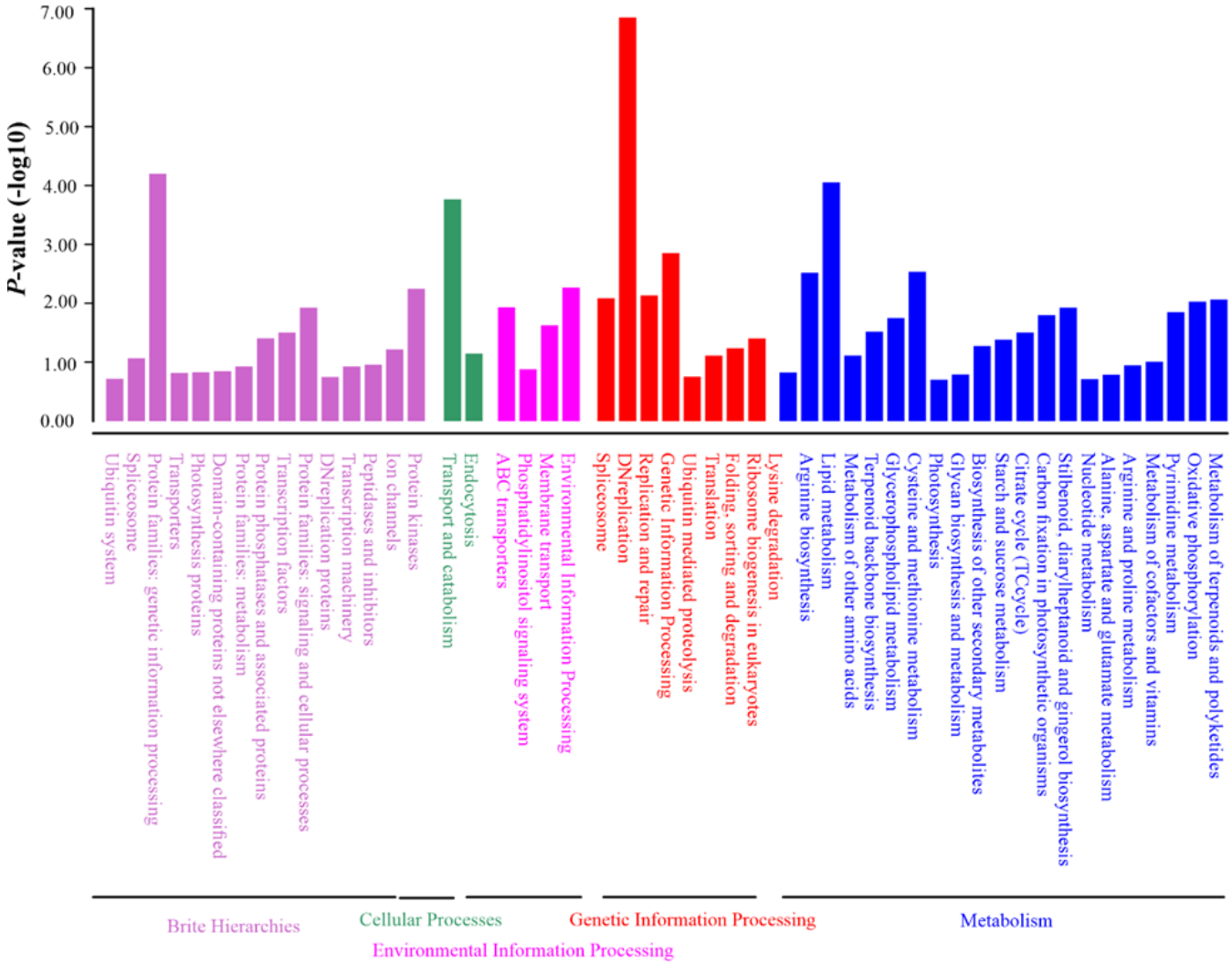

Figure 7

The biological pathways determined by KEGG analysis. The co-expressed genes of four *SlHVA22* genes having p-value less than 0.01 were subjected to KEGG analysis (see Figure 6).

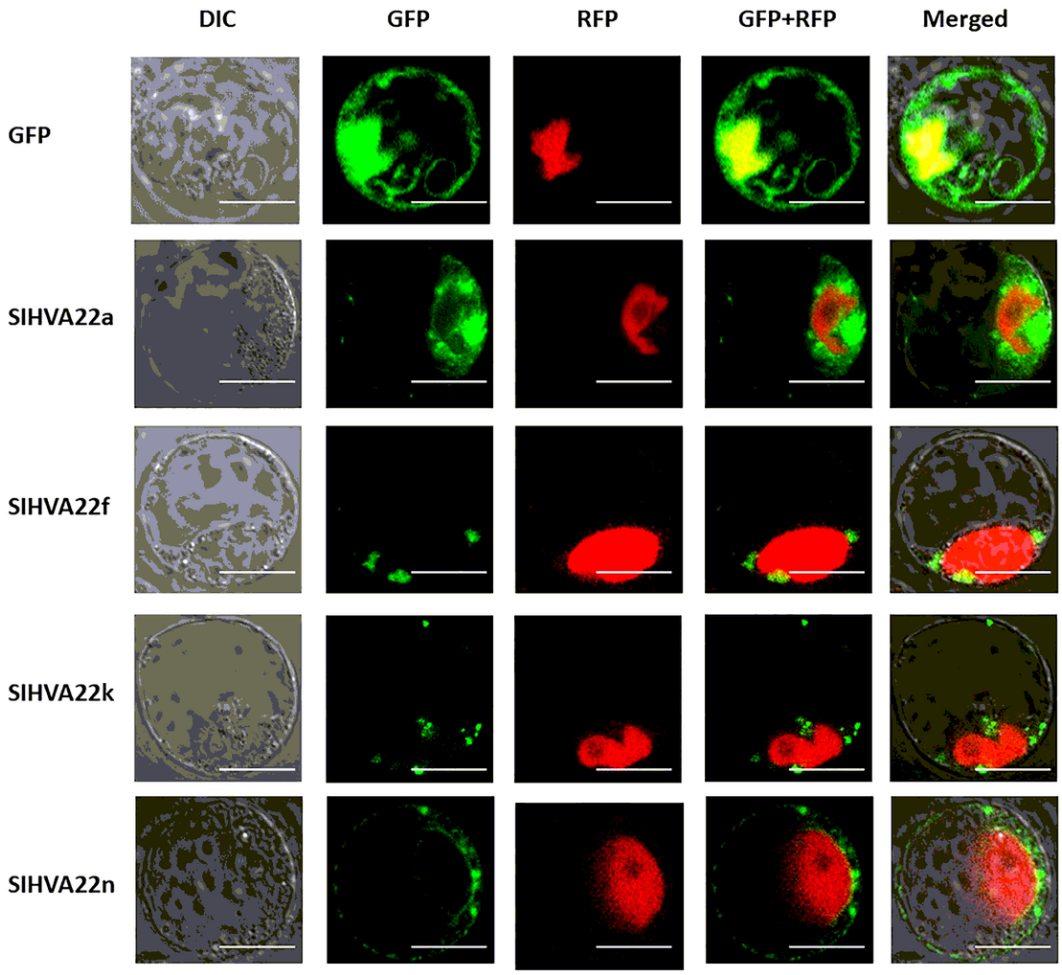

Figure 8

Sub-cellular localization of SlHVA22 proteins. SlHVA22s-SGFP fusion constructs were used to analyze the localization of SlHVA22a, SlHVA22f, SlHVA22k, and SlHVA22n, and the fluorescence signals were visualized with the confocal microscope. NLS-mRFP construct was utilized as a nuclear localization marker. Scale bars = 10 μm.

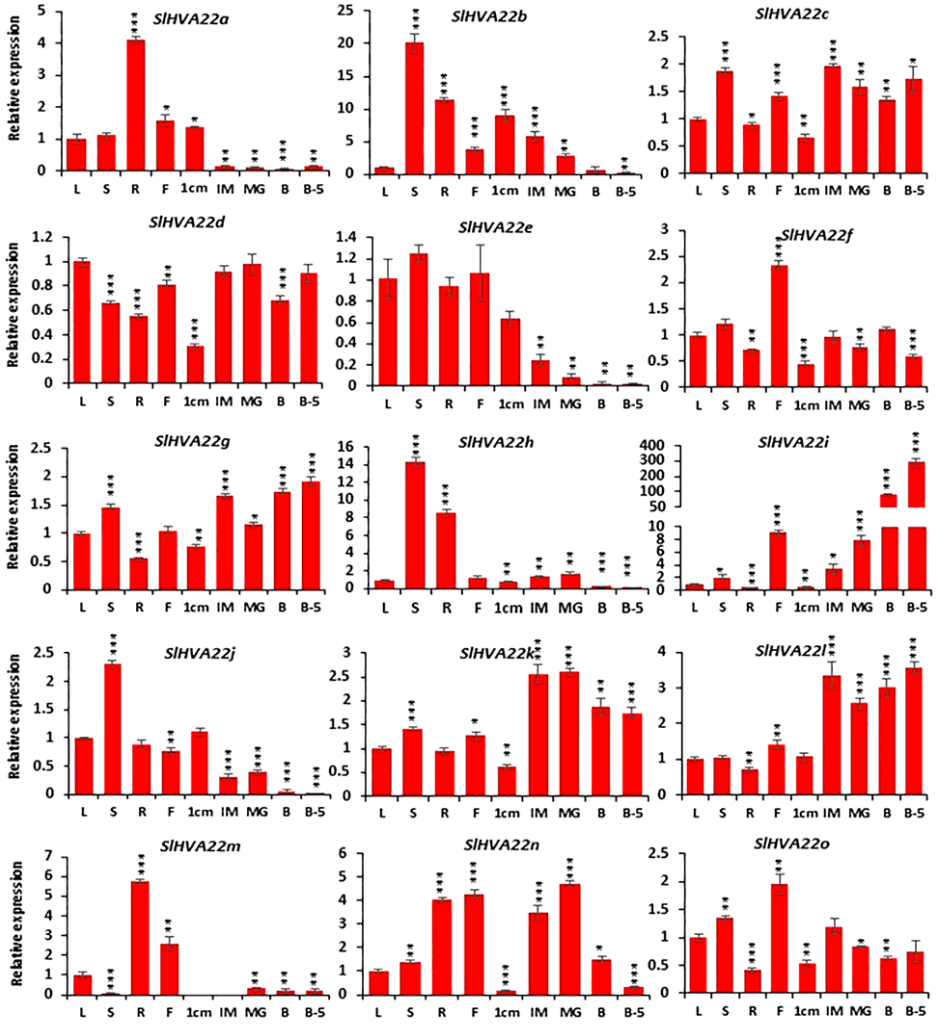

Figure 9

Expression profiles of *SlHVA22* genes in various organs: leaves, roots, stems, flower, 1 cm fruits, immature fruits (IM), mature green fruits (MG), breaker fruits (B), and fruits 5 days after breaker stage (B5). The standard deviations of the means of three independent biological replicates were represented by the error bars. The different asterisks above the bars denotes the significant variations between the control samples (leaves) and the samples harvested from the other organs, as analyzed by Student's t-test with p-values less than 0.05 for *, 0.01 for **, and 0.001 for ***, respectively.

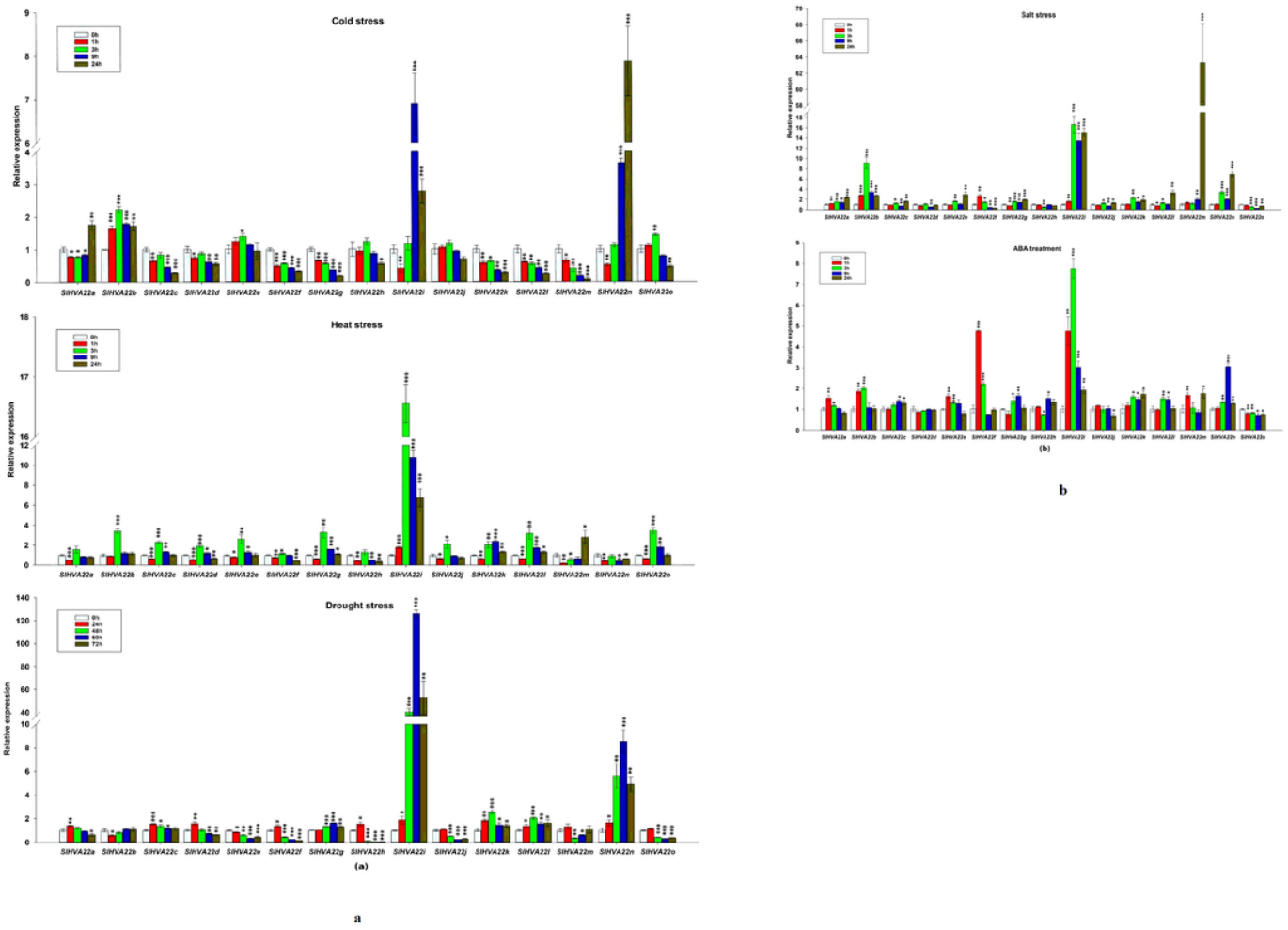

Figure 10

a-b. Expression profiling of *SlHVA22* genes under various abiotic stresses: a) cold, b) heat, c) salt (NaCl), d) drought, and e) ABA treatment. Error bars represent standard deviations of the means of three independent biological replicates of qRT-PCR analysis. The various asterisk marks (* for p-value < 0.05, ** for p-value < 0.01, and *** for p-value < 0.001) determined using student t-test indicate the statistically significant differences between the control samples (0h) and treated samples of *HVA22* genes.

Supplementary Files

This is a list of supplementary files associated with this preprint. Click to download.

- Supplementarymaterial1.docx
- Supplementarymaterial2.docx